energies

Review

MVDC Railway Traction Power Systems; State-of-the Art, Opportunities, and Challenges

Patrobers Simiyu and I. E. Davidson *

Department of Electrical Power Engineering, Durban University of Technology, Durban 4001, South Africa; PatrobersS@dut.ac.za
* Correspondence: InnocentD@dut.ac.za; Tel.: +27-31-373-2419

Abstract: Advances in voltage-source converters (VSCs), as well as their successful application in VSC-HVDC systems, have motivated growing interests and research in medium-voltage direct current (MVDC) traction power systems (TPSs) for high-speed rail (HSR) applications. As an emerging power-converter-based infrastructure, this study reviewed developments that shape two key evolving pieces of equipment—namely, high-power traction substation (TSS) converters, and power electronic transformers (PETs)—for MVDC TPS as well as prospects for smart grid (SG) applications in the future. It can be deduced that cost-effective and robust high-power TSS converters are available from hybrid modular multilevel converters (MMCs) for enhanced performance and fault-tolerance capability. In addition, silicon carbide (SiC) MMC-based PETs with input-series-output-parallel (ISOP) configuration are present for greater weight/size reduction and efficiency for MVDC rolling stock design. Finally, the implementation of a smart MVDC TPS incorporating a sophisticated railway energy management system (REM-S) based on the smart grid principles is feasible in the future, with numerous benefits. However, there are related challenges, like knowledge gaps on these technologies, the high costs involved, and lack of standardization to overcome to realize widespread future commercial deployment.

Keywords: MVDC traction power system (TPS); traction substation (TSS); PET; MMC; REM-S; smart grid (SG)

Citation: Simiyu, P.; Davidson, I.E. MVDC Railway Traction Power Systems; State-of-the Art, Opportunities, and Challenges. *Energies* **2021**, *14*, 4156. https://doi.org/10.3390/en14144156

Academic Editors: João L. Afonso, Nicu Bizon and Cristina González-Morán

Received: 10 May 2021
Accepted: 5 July 2021
Published: 9 July 2021

1. Introduction

The electric railway system is a more efficient and faster public transportation option, with higher traffic density than the diesel-powered railway system. It is also environmentally friendly in this age of demand for sustainable transportation infrastructure [1]. Electric railway traction for rapid urban/suburban transportation, as well as for high-power and long-distance applications, has a history from end of the 19th century. Over time, electric railway traction systems have undergone tremendous developments to give rise to the DC and medium voltage AC (MVAC) TPSs that exist today, with an estimated coverage of about 205,000 km worldwide. Globally, the 1.5 kV and 3 kV DC TPSs, as well as the 15 kV, 16.7 Hz and 25 kV, 50/60 Hz MVAC TPSs, are the most common [2]. Table 1 summarizes the most common electric railway traction systems in the world.

Table 1. Common electric railway traction systems in the world [2,3].

TPS	Voltage Level	Estimated Coverage (km)	Selected Countries
DC	600 V and 750 V	7650	UK
	1.5 kV	20,440	Japan, France, The Netherlands
	3 kV	68,890	Russian, Spain, South Africa
MVAC (Single Phase)	15 kV, 16 2/3 Hz	32,940	Germany, Switzerland, Norway
	25 kV, 50/60 Hz	72,110	Russian, France, China, South Africa
	11–12 kV, 25 Hz and others	3000	USA

Light rails, metros, and suburban railways operate on 0.6–1.5 kV DC TPSs with overhead lines (OHLs) or third rails. These systems have rolling stocks with power demands of less than 5 MW. For high-power and long-distance railway applications, 3 kV DC TPSs were developed. With increasing demands for high-speed rail (HSR) applications, the losses in the 3 kV DC TPSs were very large, in addition to the technical and economic challenges of realizing suitable DC circuit breakers and insulation [4]. These limitations inspired the development and deployment of the MVAC TPS to capitalize on the simplicity of the AC circuit breakers [2,5]. For technical and economic reasons, different AC voltage levels were chosen in different countries for HSR transportation. The 15 kV, 16.7 Hz MVAC TPS was adapted to mitigate the commutation phenomenon occasioned on the 50 Hz systems in Germany, Switzerland, and Norway. However, the majority of countries adopted the 25 kV, 50/60 Hz MVAC TPS, in which 1×25 kV and 2×25 kV (bi-voltage) single-phase 50/60 Hz systems are common [1,3,6]. In Table 2, the 1.5 kV and 3 kV DC TPSs—as well as the 15 kV, 16.7 Hz and 25 kV, 50/60 Hz MVAC TPSs that are the most popular—are compared based on their power supply, traction substation (TSS), OHL/feeders, and rolling stock. The advantages and disadvantages are indicated as (+) and (−), respectively.

From Table 2, most disadvantages of DC TPSs—such as more TSSs, higher traction losses, heavier OHLs, high return currents to the TSSs, and high corrosion risks—are due to low voltage supply. A high-voltage DC would combine the advantages of DC and AC, eliminating the drawbacks of DC TPSs at lower voltages. In recent years, research and development has been intensifying to explore opportunities in DC railway electrification systems beyond 3 kV [4]. Developments in voltage-source converter (VSC) technology and its successful implementation in VSC-HVDC systems have led to increasing interest and research into VSC-based medium-voltage direct current (MVDC) grids for HSR applications [7,8]. For example, the authors of [7] proposed the VSC MVDC-based railway system as a new TPS framework with greater potential than the conventional MVAC system. Further, the MVDC TPS in [8] was confirmed to be comparable to the conventional MVAC TPS, with the same distances between the TSS and the OHL cross-sections. The authors of [9] proved an MVDC TPS proposal for the French National Railways to be similar to the conventional MVAC TPS in terms of the OHL cross-section and TSS spacing. Others—as in [10,11]—demonstrated how the MVDC TPS is controllable like the conventional DC microgrid.

A new electric traction paradigm built around an MVDC system extending over a long distance feeding many traction loads is emerging. This new TPS brings various benefits, such as simpler rolling stock design, lower investment costs, higher reliability and modularity, easy integration in the AC network, and new business opportunities in the railway transport subsector [7,8]—although there are few research works on this railway infrastructure [12]. In the context of sustainable development, the MVDC system can act as an energy hub for the integration of distributed renewable energy sources (RESs), as well as energy storage systems (ESSs). In this way, the railway network operator can sell power to other consumers during low rail traffic and excess RES generation. Many more opportunities for prospective railway smart grid infrastructure are reviewed in [13,14].

Table 2. Comparison of the most common TPSs worldwide [4].

Components	1.5 kV/3 kV DC TPS	15 kV, 16.7 Hz MVAC TPS	25 kV, 50/60 Hz MVAC TPS
Power Supply/ Main Grid	+No imbalance on the utility grids. +Possible connection to weak parts of the grid. −High number of connections to main grids. +Simple power supply; no phase separation. +Low impacts on distribution network	−Dedicated railway grid; needs converters at the connection with the utility grid. +Low number of connections to the utility grid. +Simple power supply; no phase separation sections as supply is centralized. +Low impacts on distribution network	−Possible imbalance on the utility grid. −Strong electrical connection required. +Low/medium no. of connections −Complex supply; needs phase separation. −Some impacts on distribution network
TSS	−High number of TSSs (high installation, maintenance, and operation costs). −Rectifiers required (installation, maintenance, reliability). −Complex circuit breakers (CBs) and switchgears. −Complex fault detection in traction circuit. +Small TSS footprint. +Parallelled TSSs to share load; high reliability.	+Moderate noumber of TSSs +Simple CBs and switch gears. +Simple fault detection. −Large TSS footprint. +Parallelled TSSs to share load; high reliability.	+Low number of TSSs. +Simple CBs and switch gears. +Simple fault detection −Large TSS footprint. −Complex supply; less reliability
Overhead Lines (OHLs) and Feeders	+Lower isolation distances; hence, easier implementation in urban areas and tunnels. +No $jL\omega$ part of the impedance; hence. no inductive voltage drops or reactive power flow. −More losses (14–16%) in the traction circuit due to low voltage. −Heavy OHLs due to high currents; thus, higher costs. | Low-speed trains. −Heavy wear of the contact wire/pantograph; thus, high maintenance costs. −Two contact wires. +No neutral sections. +No need for adjusting phase for feeding regenerative breaking energy (RBE) back to the line −High return currents to the TSSs due to low voltage. −Uses voltage inverters to send current back to the OHLs; harmomic polution. −High risk of corrosion due to high current leaks.	−Higher isolation distances; hence, difficult implementation in urban areas amd tunnels. −Complex impedance ($jL\omega$); hence, inductive voltage drops and reactive power flow. +Low losses in the traction circuit due to high voltage. +Light OHLs; hence, lower costs due to high currents. | High-speed trains. +Low wear of the contact wire/pantograph. +One contact wire. +No neutral sections. −Necessity to adjust phase for feeding RBE to the line +Low return currents to the TSSs due to high voltage. +Uses basic transformers to send current back to the OHLs. +Low risk of corrosion due to low current leaks.	−Higher isolation distances; hence, difficult implementation in urban areas and tunnels. −Complex impedance ($jL\omega$); hence, inductive voltage drops and reactive power flow. +Low losses (4–5%) due to high voltage in the traction circuit. +Light OHLs; hence, lower costs due to high currents. | High-speed trains. +Low wear of the contact wire/pantograph. +One contact wire. −Neutral sections; hence, related power transfer interruptions, speed loss, etc. −Necessity to adjust phase for feeding RBE to the line +Low return currents to the TSSs due to high voltage. +Uses basic transformers to send current back to the OHLs. +Low risk of corrosion due to low current leaks.
Rolling Stock	+No onboard transformer; hence, lighter rolling stock. +No onboard rectifier, as inverter directly connected to the OHLs; hence, lighter and more reliable rolling stock. −Converter complexity, interaction problems, and reliability. −Complex CBs.	−Very heavy and bulky onboard transformers; hence, heavy rolling stock. −Need for onboard rectifiers. −Converter complexity, interaction problems, and reliability. +Simple CBs.	−Heavy and bulky onboard transformers; hence, heavy rolling stock. −Need for onboard rectifiers. −Converter complexity, interaction problems, and reliability. + Simple CBs.

Therefore, this paper outlines the MVDC TPS as the state-of-the art electric railway infrastructure, and explores opportunities at the component, converter and system levels as a converter-based system, and related challenges. Section 2 gives a description of the state-of-the-art MVDC TPS. In Section 3, opportunities and challenges faced by the MVDC TPS at the component, converter and system levels are outlined, while the conclusions drawn are presented in Section 4.

2. State-of-the-Art MVDC TPS

2.1. Overview of the MVDC TPS

Research into DC opportunities for HSR applications other than the 3 kV DC TPS—which is at its operational and technological limits—have identified low-voltage DC as the main hindrance [4,9]. Thus, researchers explored other avenues, such as the first proposal on the HVDC TPS by [15], in which a 30 kV_{dc} classical HVDC transmission system with a rectifier TSS comprising a transformer, a 12-pulse controlled thyristor converter, and filters including fast protection equipment for preventing overcurrents was considered. The HVDC inverter station was designed to be part of the locomotive drive unit consisting of an HV inverter, a high-frequency transformer, a four-quadrant rectifier, a three-phase voltage source inverter, and three-phase asynchronous motors. Although the proposal was a realistic concept from the mature HVDC technology, the onboard HV inverter control was challenging although the paper never provided such details. Further developments in VSC technology motivated the authors of [7] to propose a new multiterminal MVDC TPS as the alternative for the 3 kV_{dc} and the conventional MVAC TPSs in HSR applications. For the existing 1.5 and 3 kV DC TPSs, the authors of [9] provided a cost-effective proposal for upgrading and transitioning to the novel MVDC TPS.

Figure 1 shows a generic MVDC TPS structure. The VSC-based TSSs derive power from the HVAC feeders, depending on the train traction loading. The track-side DERs along the catenary traction line—such as RESs and ESSs—can be integrated easily to enhance utility supply reliability and voltage regulation [7,8]. The study by [16] ascertains that an HVDC system can supply the MVDC TPS. The MVDC system at lower voltages can feed urban railway systems [6], electric vehicle (EV) charging stations [17], urban centers [18], etc.

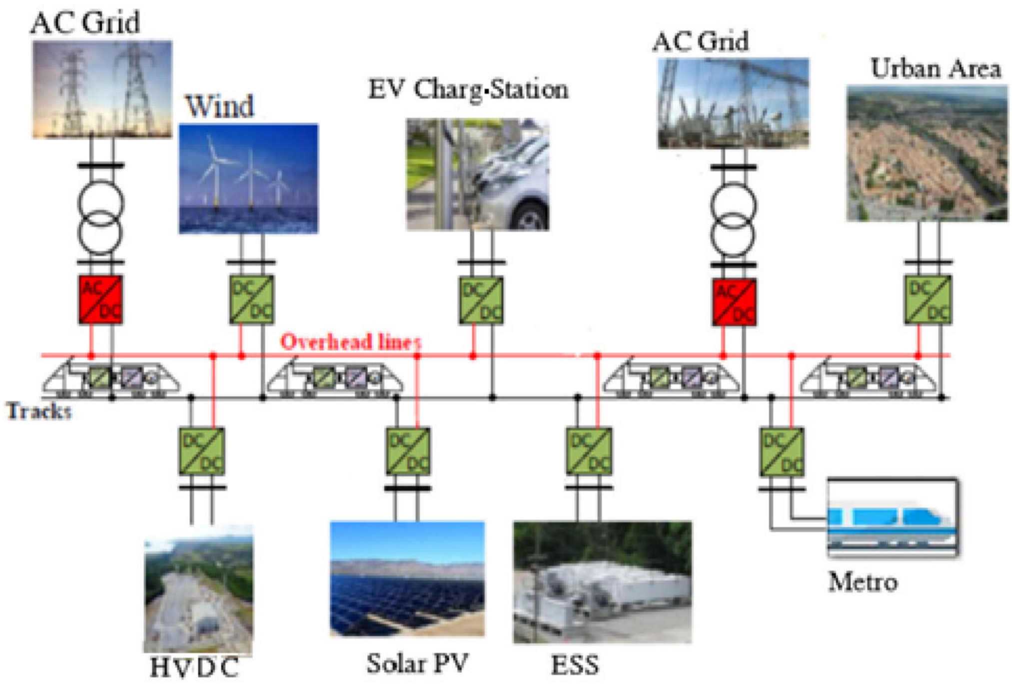

Figure 1. A generic structure of the multiterminal MVDC TPS.

2.2. MVDC TPS as an Enhanced DC TPS

The use of a higher value than 3 kV_{dc}—for instance, 5–25 kV_{dc}—could encompass the advantages of DC and MVAC TPSs, as well as facilitate new opportunities [4]. Different researchers have used different values within the voltage range, depending on their research purposes. For instance, the French National Railway investigations for upgrading their 6000 km 1.5 kV_{dc} TPS to MVDC used 9 kV_{dc} [9], while [8], in a similar setup, studied 7.5 kV_{dc}, 9 kV_{dc}, and 10.5 kV_{dc}. On the other hand, the authors of [7,10,11] and [19] considered 24 kV_{dc}. Standard voltages shall be a key design consideration for a commercial MVDC TPS for widespread application and interoperability [4].

High DC voltage will necessitate fewer TSSs than the DC TPS. The TSS architecture would take more power from the utility, without any imbalance. The higher voltage levels reduce the current levels, enabling lighter OHLs with reduced installation and maintenance costs. Table 3 summarizes the enhanced features of the MVDC TPS vis-à-vis the two most popular TPSs worldwide, based on the power supply, TSS, OHL/feeders, and rolling stock. The advantages and disadvantages are indicated as (+) and (−), respectively.

Table 3. Comparison of the MVDC TPS as an enhanced system and the 25 kV, 50/60 Hz MVAC TPS [4,6–8,15,20,21].

Components	3 kV DC TPS	MVDC TPS (Enhanced to 5–25 kV)	25 kV, 50/60 Hz MVAC TPS
Power Supply/Main Grid	+No imbalance on the utility grids/distribution network. +Possible connection to weak parts of the grid. −High number of connections to main grids. +Simple power supply; no phase separation.	+No imbalance on the utility grids/distribution network. +Possible connection to weak parts of the grid. +Low number of connections to the utility grid. +Simple power supply; no phase separation. +Possible railway smart grid.	−Possible imbalance on the utility grid/distribution network. −Strong electrical connection required. +Low/medium number of connections −Complex supply; needs phase separation.
TSS	−High number of TSSs (high installation, maintenance, and operation costs). −Rectifiers required (installation, maintenance, reliability). −Complex circuit breakers (CBs) and switchgears. −Complex fault detection in traction circuit. +Small TSS footprint. +Paralleled TSSs to share load; high reliability.	+Low number of TSSs −Complex CBs and switch gears. +Possibility of using TSS converters to control short circuit currents. −Complex fault detection in traction circuit. +Small TSS footprint. +Paralleled TSSs to share load; high reliability.	+Low number of TSSs. +Simple CBs and switch gears. +Simple fault detection −Large TSS footprint. −Complex supply; less reliability

Table 3. *Cont.*

Components	3 kV DC TPS	MVDC TPS (Enhanced to 5–25 kV)	25 kV, 50/60 Hz MVAC TPS
Overhead Lines (OHLs) and Feeders	+Lower isolation distances; hence, easier implementation in urban areas and tunnels. +No jLω part of the impedance; hence, no inductive voltage drops and reactive power flow. −More losses (14–16%) in the traction circuit due to low voltage. −Heavy OHLs due to high currents; thus, higher costs. ∣ Low-speed trains. −Heavy wear of the contact wire/pantograph; thus, high maintenance costs, −Two contact wires. +No neutral sections. +No need for adjusting phase for feeding regenerative breaking energy (RBE) back to the line −High return currents to the TSSs due to low voltage. −Uses voltage inverters to send current back to the OHLs; harmonic polution. −High risk of corrosion due to high current leaks.	−Higher isolation distances; hence, difficult implementation in urban areas and tunnels. ∣ HSR +No (jLω); hence, inductive voltage drops and reactive power flow. +Low losses in the traction circuit due to high voltage. +Light OHLs due to lower current. ∣ High-speed trains. +Low wear of the contact wire/pantograph. +One contact wire. +No neutral sections. +No need for adjusting phase for feeding RBE to the line, i.e., uses reversible converters. +Low return currents to the TSSs due to high voltage. +Uses basic transformers to send current back to the OHLs. +Low risk of corrosion due to low current leaks.	−Higher isolation distances; hence, difficult implementation in urban areas and tunnels. ∣ HSR −Complex impedance (jLω); hence, inductive voltage drops and reactive power flow. +Low losses (4–5%) due to high voltage in the traction circuit. +Light OHLs; hence, lower costs due to high currents. ∣ High-speed trains. +Low wear of the contact wire/pantograph. +One contact wire. −Neutral sections; hence, related power transfer interruptions, speed loss, etc. −Necessity to adjust phase for feeding RBE to the line +Low return currents to the TSSs due to high voltage. +Uses basic transformers to send current back to the OHLs. +Low risk of corrosion due to low current leaks.
Rolling Stock	+No onboard transformer; hence, lighter rolling stock. +No onboard rectifier, as inverter directly connected to the OHLs; hence, lighter and more reliable rolling stock. −Converter complexity, interaction problems, and reliability. −Complex CBs. +Mature rolling stock technology	+Light onboard PETs; hence, lighter rolling stock. +No onboard rectifier; thus, ligher rolling stock. −Converter complexity, unknown interaction problems, and reliability. −Complex CBs and protection circuit to limit fault currents in onboard PETs. −Immature rolling stock technology	−Heavy and bulky onboard transformers; hence, heavy rolling stock. −Need for onboard rectifiers. −Converter complexity, interaction problems, and reliability. +Simple CBs. +Mature rolling stock technology

From the comparison in Table 3, the MVDC TPS has some "grey areas" where research and development are yet to breakthrough to fully compete with MVAC TPS. As an emerging technology, developing—for example—suitable circuit breakers, fault detection schemes, power electronic transformers (PETs), power converters, etc. is crucial in hastening its technological competitiveness. In particular, the PETs for railway applications are not well established, with some challenges regarding protection, isolation, and reliability to be addressed before the technology reaches maturity [22–25]. An MVDC circuit breaker for protection against DC-side faults whose technology is not very mature [26] will be required in the onboard circuitry containing the PETs, amongst other MVDC circuits. High-power bidirectional MVDC converters are still underway, with Siemens having made significant progress through its first commercial MMC-based MVDC converter in [27], which will likely stimulate more MVDC grid solutions. The switching characteristics of PETs and high-power MVDC converters can cause significant electromagnetic interference (EMI) within the rolling stocks, TSSs, and the space along the OHLs/tracks. However, investigations on such EMI phenomena in MVDC TPSs are quite limited. A study shows that operational speed and DC voltage increase resulted in EMI effects on the 25 kV_{ac} Beijing–Zhangjiakou HSR line model modified to an MVDC TPS [28].

On the other hand, there are new opportunities associated with the MVDC TPS; for instance, RESs such as wind and photovoltaic (PV) power can be efficiently integrated into the MVDC in order to reduce the system's peak load and, hence, the costs on the host AC utility grid [7]. Excess generation from the RESs can be fed back to the utility grid though any adjacent reversible TSSs. Track-side ESSs such as batteries, supercapacitors, and flywheels can also be integrated for storing excess energy from the RESs and some RBE, as well as for energy balancing in the system [29,30]. A combination of PV and battery storage with an appropriate control strategy can also provide a novel catenary voltage regulation and stray current mitigation, without any ESS sizing constraints, as demonstrated in [19]. The novel stray current mitigation scheme can manage the cathodic corrosion challenges of metallic structures embedded near the TPS. Fast EV-charging infrastructure can be incorporated via existing TSSs or OHLs to increase the utilization rate of the MVDC TPS. Additionally, train RBE can be fed back to the AC utility grid or utilized to charge EVs, significantly decreasing the system's energy consumption [17,31]. Further, low-power rail systems such as trams, metros, and suburban railways can be integrated through a PET that offers high power density and high efficiency as well as bidirectional power flow capability to feed excess power from the catenary network [6,32,33]. Last, but not least, the authors of [18] ascertained a higher economic feasibility of MVDC grids over low-voltage AC systems for urban power supply. Thus, an MVDC TPS can be an energy hub connected to provide excess power supply to a set of urban DC homes or some remote adjacent village microgrids, with numerous advantages over AC supply [34]. Similarly, the DC power can be supplied to offices and commercial facilities with existing cables at higher efficiency [35,36]. This massive railway infrastructure with distributed loads (trains, EVs, urban and rural residents) sources (distributed RESs) and ESSs necessitates the application of smart grid (SG) principles, as in [37]. The smart MVDC TPS concept can provide greater energy and cost savings as well as reduced supply uncertainties due to highly level local and global optimization [13].

2.3. MVDC TPS Control

Typically, an MVDC TPS is synonymous with a conventional DC microgrid; hence, related control concepts apply [11]. When the train travels along the catenary line, its power and track rail resistances with respect to departure and arrival stations keep changing; hence, its power supply/current also change [38]. The TSS near the train provides more power compared to the one further away. As such, unless proper power/current sharing amongst the parallel VSC-based TSSs is ensured, the RESs and the stiff utility grid can reach their maximum limits. Thus, an effective coordination control scheme is necessary to ensure effective power sharing amongst the paralleled TSSs [10]. In the literature, a number of centralized and distributed DC voltage primary control schemes—such as master–slave and droop-based control, respectively—have been explored in order to achieve proper power sharing in DC systems with similar parallel building blocks. Generally, the droop-based control strategies are reliable, flexible, and expandable schemes with high dynamic performance and with minimal communication needs, suitable and adaptable for the stable and secure operation of VSC-based MVDC grids [39]. The conventional droop control was proposed for primary VSC-based TSS controllers to maintain the system's DC voltage [7], but was found to be prone to severe catenary voltage fluctuations, as well as inaccurate current sharing due to the unique train traction load dynamics. Therefore, an improved droop control scheme that simultaneously applies voltage shifting and load current feed-forward control approaches for enhancing catenary network voltage was proposed in [10]. In [11], an adaptive droop control strategy was proposed for more effective current sharing amongst the TSSs at permissible catenary voltage. It should be noted that the above studies neglected RBE. Although there are few studies on adaptive droop control in MVDC TPSs, their increasing application in DC systems as reported in [39–41] heralds greater opportunities for innovations to realize excellent DC voltage regulation and power sharing in MVDC TPS.

A hierarchical control scheme involving a combination of primary and secondary control layers is highly popular in DC grid operation control. The secondary controller dictates the reference point of the primary controller based on the optimal power flow (OPF), subject to certain techno-economic constraints [42–44]. In this way, an efficient hierarchical control scheme considering RBE in a DC TPS with reversible TSSs was proposed for DC voltage regulation and power sharing in [45]. The droop-based control was implemented at the primary level, whereas at the secondary level, the droop settings were determined using the AC/DC sequential OPF algorithm based on the Newton–Raphson method, as shown in Figure 2a. The secondary controller, based on nonlinear steady-state models, is an open loop with limited feedback, while the primary controller based on linear dynamic models uses feedback to realize hierarchical control optimization. In some cases, the secondary controller can take the form of a dedicated railway energy management system (REM-S), as illustrated in Figure 2b. The REM-S not only supervises the speed of the trains, but also performs state estimation, automatic power and voltage control, and security assessment, as well as regulating the transmission network's impact based on transmission system operator reference signals [7]. A more intelligent REM-S is proposed as a smart grid architecture model, where the TPS, trains, and DERs—including track-side ESS and external consumers—are dynamically coordinated to realize optimal system energy usage [37]. Centralized and decentralized optimization algorithms were then developed, and their functionality and efficiency evaluated by way of simulations in offline and online real case studies on a 3 kV_{dc} TPS in Spain [46]. The REM-S software sets presented in [47] are the first prototype of the REM-S concept and architecture to be validated in real-time rail operation.

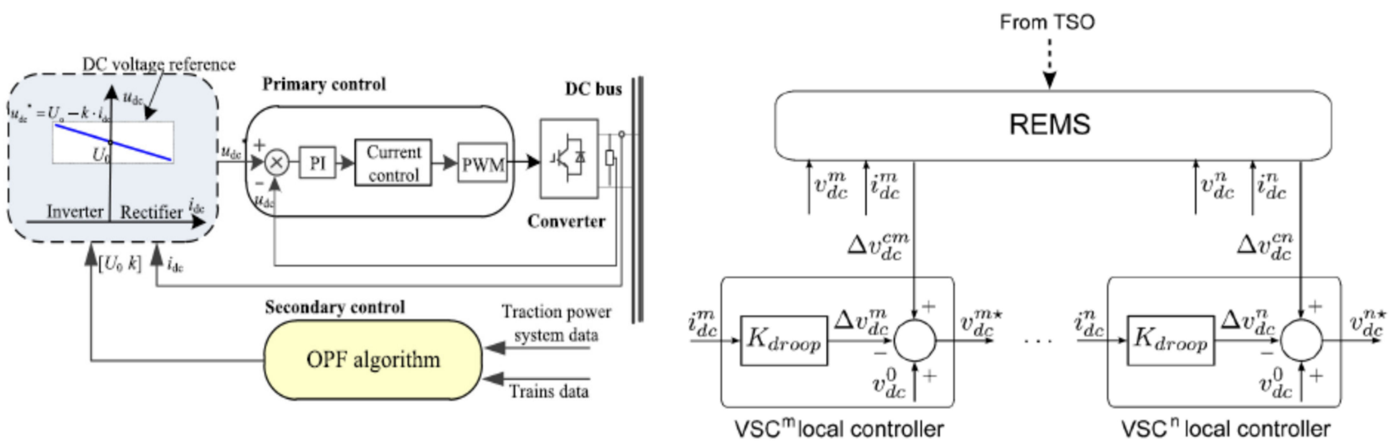

(**a**) (**b**)

Figure 2. TPS control: (**a**) hierarchical control [45] and (**b**) REM-S [7].

3. Key Opportunities and Challenges

As pointed out in the previous section, the MVDC TPS is technically, operationally, and economically relevant for HSR applications, with a combination of benefits from the AC and DC TPSs [4,8]. As a power-converter-based system still evolving in certain aspects, there are some "gaps" that ongoing research and development can fill to boost confidence as a competitive system of the future [20]. Thus, this study explores trends along the converter value chain that inspire MVDC TPS development and related challenges. The opportunities and challenges are explored at the component, converter, and system levels.

3.1. Component Level

In MVDC TPS operation, very efficient and reliable high-power TSS converters are desirable. Additionally, equipment such as DC–DC converters or PETs should be ragged, compact, and with high power density. Innovations in the "building blocks" of this converter equipment—such as wide-bandgap (WBG) semiconductors and medium-frequency transformers (MFTs)—are useful in realizing the required MVDC TPS services.

3.1.1. Wide-Bandgap (WBG) Semiconductors

The silicon (Si) technology that has dominated the commercial semiconductor device arena is reaching its material limits regarding blocking voltage, operating temperature, conduction and switching characteristics that impede higher power conversion [48]. However, WBG semiconductor devices—like silicon carbide (SiC) and gallium nitride (GaN) semiconductors—can decrease the switching losses by 50%, increasing efficiency to about 95–99%, as well as operating at higher voltages, switching frequencies, and harsh environments. Figure 3 compares the key material characteristics of Si and WBG semiconductor devices, in which the WBG devices lead Si in high-voltage, high-temperature, and high-frequency switching operations. Thus, the WBG devices are attractive in developing smaller, lighter, and more cost-effective power converter equipment with reduced passives and cooling systems [48,49].

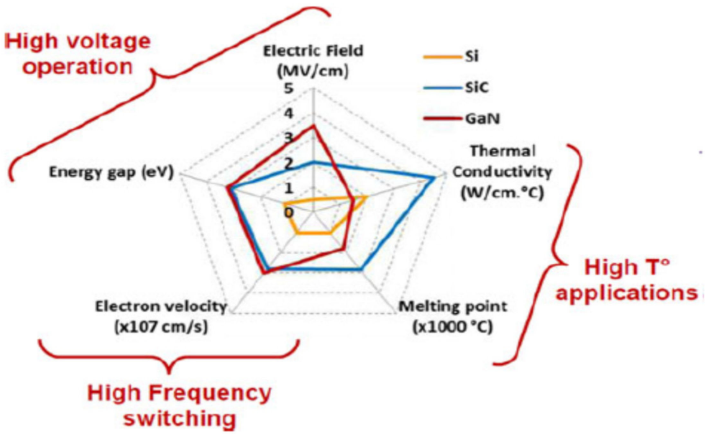

Figure 3. Key material properties of Si and WBG semiconductor devices [50].

The major drivers for increasing WBG utilization are the need for energy efficiency, reduction in size/weight, capability of withstanding high operating temperatures and switching frequencies, and low costs. Table 4 illustrates a comparative analysis of WBG market drivers for selected applications. In traction applications, the decrease in the size and weight of WBG-based converters is important in realizing a lighter locomotive that can move at higher speeds. Stationary applications—such as power supply UPS, PV, wind generators, and motor drives—have less consideration for size and weight reduction [49,51].

Currently, the WBG semiconductor market is focused on SiC technology, with the market share dominated by companies from the USA, Japan, Europe, and China [49,51]. SiC is more popular for high-power applications due to having more maturity than GaN in bulk material growth and wafer advances, as well as being operational at higher breakdown voltages and currents [50,52]. Twenty-four SiC MOSFETs and twelve Schottky diodes were assembled in a 10 kV half H-bridge power module that was used to design and demonstrate a 13.8 kV to 465/$\sqrt{3}$ V, 1-MVA single-phase solid-state power substation. At 855 kVA, the power station recorded 97% efficiency, 70% weight reduction and 50% reduction in size compared to the conventional 60 Hz transformer [53]. In 2015, a 3.3 kV/1500 A power module comprising 16 SiC MOSFETs and 16 SiC Schottky barrier diodes was mounted onto a world-first all-SiC traction inverter; the study demonstrated a decrease in switching loss by 55% compared to a corresponding Si inverter [54]. The first HSR traction system on the Tokaido Shinkansen train line in Japan—based on SiC—increased the compactness of the conversion system's width by half, and achieved axial length reduction of the traction motor by 10%. The total weight of the traction system reduced by 20%, with even more prospects for future reduction [55]. A PET from a combination of 15 kV SiC MOSFETs and Schottky junction barrier diodes achieved a peak efficiency of 97% [56].

Table 4. Market drivers for selected WBG applications [49,51].

Market Driver	Power Supply	UPS	PV	Wind	Motor Drives	Rail	H/EV	Key
Efficiency	●	◒	●	●	●	◒	●	● High
Weight/Size	◒	○	○	◒	◒	●	●	◒ Moderate
Operating Temperature	○	◒	○	○	●	◒	●	○ Low
Switching Frequency	○	○	○	○	◒	◒	●	
Cost	◒	●	●	◒	◒	○	●	

Theoretical studies indicate that candidate SiC MOSFETs are within 10–15 kV breakdown voltage, whereas SiC-IGBTs have the potential for use below and above 15 kV due to better on-state performance [48]. Comparing two 15 kV SiC devices shows that SiC MOSFETs are more favorable for higher switching frequencies at the same dv/dt than SiC IGBTs. However, both have almost the same total switching losses at 25 °C, whereas SiC-IGBTs have higher losses at higher junction temperatures [57]. In [58], the 10 kV and 15 kV SiC MOSFETs were proved to possess immense potential to significantly impact the system performance, footprint, weight, high-temperature reliability, and cost of next-generation power conversion and transmission systems. Currently on the market, Hitachi has 3.3 kV full-SiC and hybrid-SiC IGBT modules [59], while Toshiba has 3.3 kV SiC MOSFETs [60], among other manufacturers with their own products.

A full-bridge MMC based on 1.7 kV SiC MOSFETs is proposed for an MVDC ship power system. A fault current control scheme is proposed for the MMC with the power electronic building blocks. The simulation and experimental results demonstrate that the MMC can clear DC fault current when a DC short circuit occurs, as well as restoring service when the fault is isolated [61]; this is a significant step in achieving appropriate high-power MVDC converters for TSSs.

There are great prospects for SiC devices for urban railways and HSR applications due to their higher efficiency, enhanced thermal properties, and higher switching frequencies with lower losses [51]. These are desirable features that shall be necessary for MVDC TPS applications. In this way, the integration of SiC in TSS converters, PETs, variable frequency drives, and auxiliary systems will not only increase conversion efficiency but also reduce the cooling system's requirements, locomotive weight, and power demand. The use of these semiconductor devices allows for the improvement of existing power converters and the development of new ones that account for increased power conversion efficiency as well as better power utilization. In spite of this potential, WBG devices constitute a very small portion of the power electronics market, due to having about 10 times the cost of silicon (Si) discretes and less mature technology than Si and hence, reliability concerns and lower production. Moreover, the optimal design of packaging, passives, and power converter equipment's system level topology is yet to be realized [49]. As demand for WBG integration increases, advances in technology will strive to lower the related costs and boost production volumes [48].

3.1.2. Medium-Frequency Transformers (MFTs)

The magnetic components of the PET systems are their bulkiest part; hence, many research efforts have focused on size and weight reduction. Unlike hard magnetic materials such as Si–steel that are suitable for low-frequency transformer (LFT) cores, soft magnetic materials are used in MFTs (>400 Hz). Table 5 shows typical transformer core materials; the amorphous and nanocrystalline cores have high saturation flux density, high permeability, low loss, and higher continuous operating temperatures, and are thus appropriate for high-frequency and high-power applications [33,62]. These core materials are preferable to the widely used Si–steel laminations and ferrite, mainly for LFTs, but their costs are higher, including a complex and expensive manufacturing process [33,63].

Table 5. Typical transformer core materials [33].

Features	Si-Laminations	Ferrite	Amorphous	Nanocrystalline
Saturation Flux Density	1.7–2.0 T	0.3–0.5 T	0.8–1.5 T	1.1–1.3 T
Permeability	2 k–20 k	1.5 k–15 k	6.5 k–8 k	20 k
Energy Loss	High	Modest	Low	Lowest
Continuous Operation Temperature	120–130 °C	100–120 °C	120–150 °C	120–180 °C
Curie Temperature	730 °C	220 °C	>350 °C	>550 °C
Cost	Low	Moderate	High	Highest
Thermal Conductivity	Very high	High	Low	
Large Cores?	Yes	No	Yes	
Other	Very robust; Flexible design	Very brittle; High tolerance	Very hard; Complicated to process; Expensive cuts	

In addition to the selection of core materials, the design of the MFT also depends on winding configuration and the core structure. Litz wires are preferable for MFT windings due to higher copper density and space utilization. The shell structure is the most appropriate transformer core configuration from the thermal point of view [62]. MFTs show higher core losses, larger harmonics, and abnormal eddy losses due to nonsinusoidal excitation; thus, they become severely overloaded. In this way, optimal MFT design is necessary when considering their transient thermal behavior for an effective cooling system [64].

A proposed optimal MFT design given in [65] is shown in Figure 4. A summary of the design procedure is outlined in the following steps:

i. The transformer system's level characteristics are defined to a circuit calculator.
ii. Conductor, isolation, and core material properties are introduced.
iii. The geometry of the transformer parts is parameterized with respect to the free variables that are varied during the designing process in order to realize an optimal design.
iv. The core, windings, and insulation losses are calculated considering high-frequency (HF) effects.
v. The temperature of the components is estimated using thermal models, and the isolation level reached is calculated. If both parameters meet the requirements, the values are stored and another set of parameters is selected for the next design process.
vi. Once all of the combinations of free parameters are tested, the optimal set of free parameters for the given optimization process (i.e., efficiency or power density) can be extracted. A new optimization process can be initiated with a different selection of core materials for comparison.

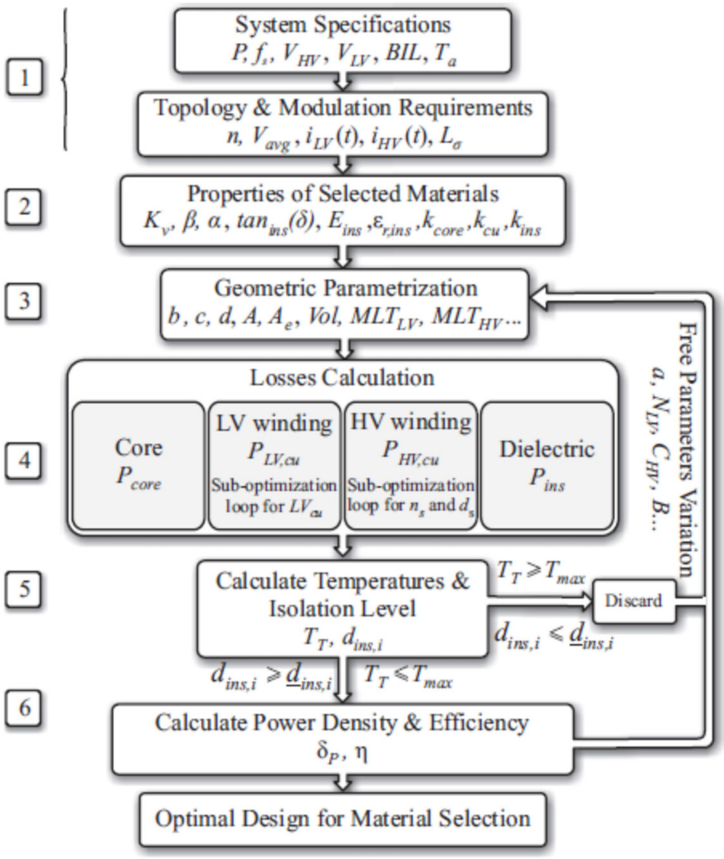

Figure 4. MFT optimal design [65].

In [65], the isolation was given special attention due to its influence over other design parameters. A more comprehensive optimization routine is given in [66] for designing an optimal 166 kW/20 kHz PET prototype with 99.47% efficiency at 44 kW/dm^3 power density. In terms of notable railway traction applications, Bombardier developed an 8-kHz, 3-MW MFT prototype from a nanocrystalline core for a 15 kV, 16.7 Hz MVAC TPS PET in [67], whereas ABB developed 9 MFTs from C-cut nanocrystalline cores for a similar PET [68] that shows development potential for MVDC TPSs.

Despite the advantages of MFTs in creating a large reduction in the size and weight of magnetic components—especially on the bulky transformer—there are several challenges to realizing optimal MFT design for railway traction applications, which require further interrogation. Designing an effective, low-cost, reliable cooling system is very difficult in thermal modelling. The prevalence of nonsinusoidal voltage and current waveforms necessitates more complex design methods [33,62]. Further investigation into insulation materials that can withstand medium-frequency voltage stress and MFT construction optimization—amongst others—is also necessary [64].

3.2. Converter Level

High-power converters can serve as an important component of the TSS, interfacing the utility three-phase supply and AC-based DER, as well as being integrated in the traction drive to feed the traction motors. The converters should be able to withstand short traction overloads. Reversible VSC-based TSS converters are desirable for feeding regenerative braking energy back to the utility supply. The review of VSCs shows that they have numerous applications that can help identify suitable converter solutions for MVDC TPS applications. On the other hand, the PET is a 'new generation' equipment that offers weight and size reduction as well as other functionalities—unlike the conventional, bulky, low-frequency transformer (LFT). PETs have a long history in rolling stock traction applications in MVAC TPSs; hence, a review will help to realize possible innovations for MVDC TPS applications. The application of PETs in the integration of DC-based DERs and loads will not be considered.

3.2.1. Voltage-Source Converters (VSC)

In the recent past, Si-IGBT-based VSCs with DC capacitor storage in the DC link have gained rapid market penetration; Figure 5 shows the main classes of the VSCs. The two-level converter is the standard VSC limited to $\frac{+V_{DC}}{2}$ and $\frac{-V_{DC}}{2}$ levels only in each phase at the AC side. Two-level converters have been implemented for high-power applications in the ±1500 kV VSC-HVDC, in which better controllability was realized with PR than with PI controllers in rejecting voltage grid disturbances [69]. In traction applications, the two-level IGBT rectifier operates at unity power factor and low harmonic pollution, as well as facilitating regenerative braking energy recuperation. However, its 4x higher losses and 2.5x higher semiconductor costs than the thyristor-controlled rectifier, along with its inability to limit DC short circuit currents, illustrates why the latter is more applicable in conventional DC TPSs [70].

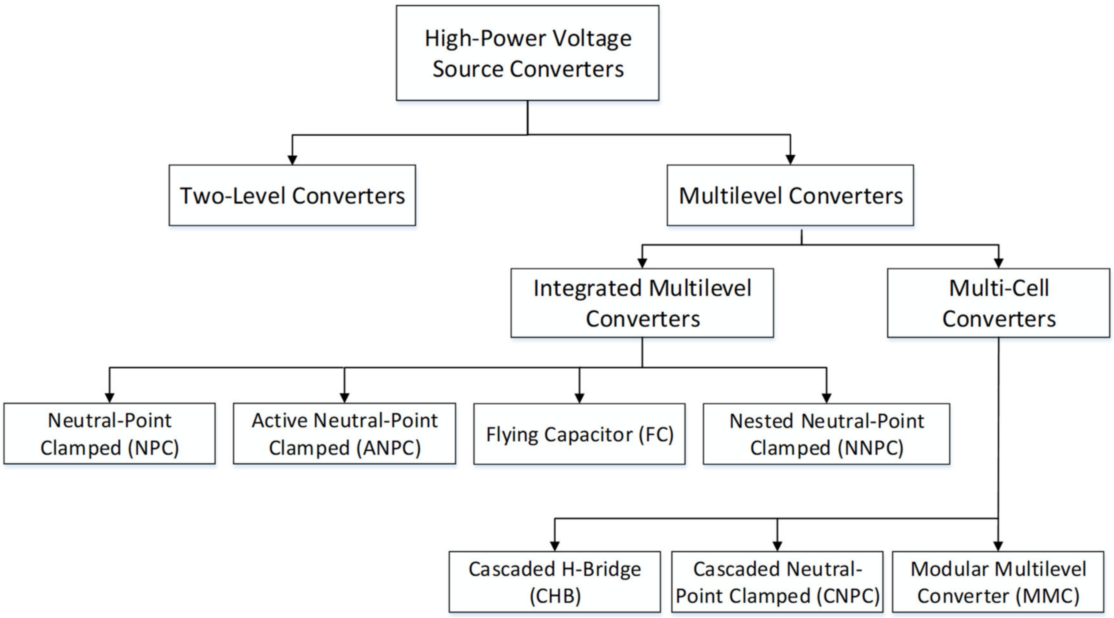

Figure 5. VSC classes [71].

The development of multilevel VSCs arrived as a new solution in place of two-level converters for high-power applications. In relation to two-level converters, multilevel converters generally have staircase voltage waveforms on the AC side, with lower harmonic distortion, near-sinusoidal currents at the AC side, lower voltage stress on IGBTs, higher efficiency, and smaller filters. Multilevel VSCs are divided into integrated (monolithic) and multicell converters, as detailed in [71]. The integrated and multicell converters that can handle 2.3–4.16 kV do not have a modular structure; hence, a large number of IGBTs are installed, necessitating a complex and costly design. Additionally, challenges of reliability and voltage balancing exist because of the high component count. As a result, the cascaded H-bridge (CHB), cascaded neutral-point clamped (CNPC), and modular multilevel converter (MMC) were constructed using a modular topology to achieve higher operating voltages of 6.6–13.8 kV using Si-IGBTs to solve this problem [71,72].

The complexities involved when implementing bidirectional AC/DC converters from CHB and CNPC inspired the emergence of MMCs [71]. MMCs are characterized by increased modularity, scalability to any power or voltage level, filter-free high-power-quality operation, transformerless operation, high efficiency, fault tolerance capability, the absence of DC link capacitance, and lower electromagnetic interference [73,74]. Figure 6 shows a generalized schematic diagram of a three-phase MMC. Typically, the MMC comprises two arms per phase leg, each consisting of *n* identical series-connected submodules (SMs) and a series arm inductor. The SMs in each arm are individually and selectively controlled to generate the required AC phase voltage. The inductor suppresses the inrush currents during startup and the circulating currents when in steady-state operation. The upper (lower) arms of the three phase legs are connected to the positive (negative) bar, and the total voltage between the two arms equals V_{dc} [73,75].

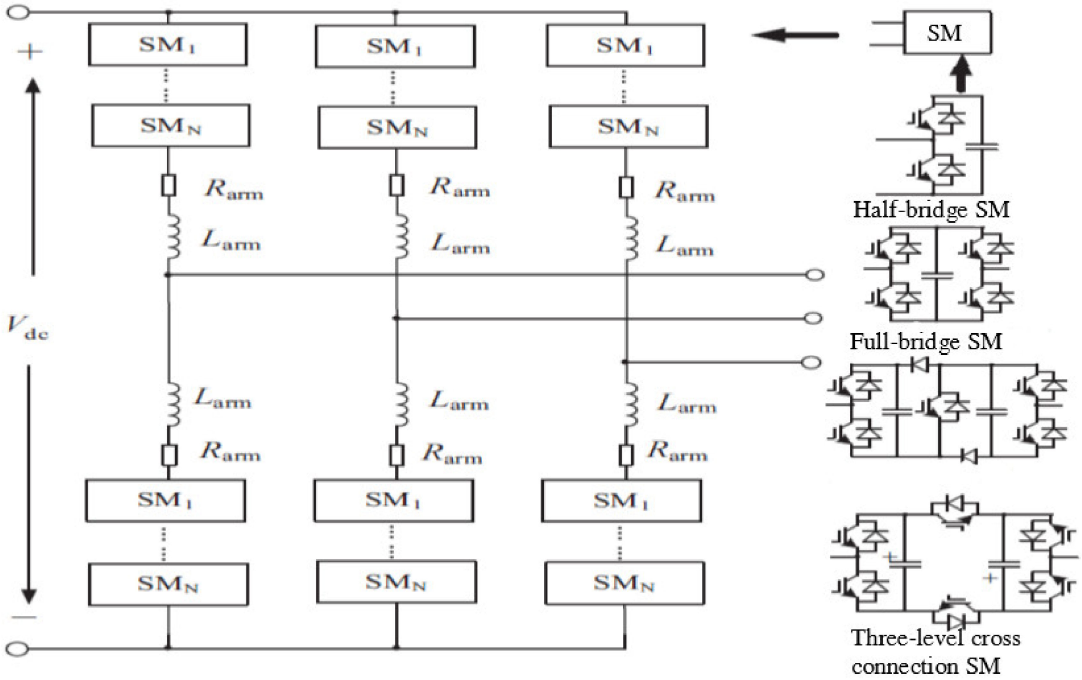

Figure 6. Generalized schematic diagram of a three-phase MMC.

The MMC based on the half-bridge (HB) SMs is the most popular topology for medium and high-voltage applications; this is due to it having only two switches and one floating capacitor, resulting in a simple design and control. During normal operation, only one switch is "ON", presenting low power loss, whereas the output voltage consists of two voltage levels of "0" and "+V_c". The positive voltage levels alone cannot support bipolar operation and DC fault blocking. Consequently, during DC faults, HB SMs cannot block fault currents on the AC side. Thus, opportunities for other SMs such as full bridge (FB), unipolar full bridge (UFB), clamped double circuits (CDC), and the three-level converter circuit (3LCC)—three-level NPC or three-level FC—as well as the five-level cross-connected (5LCC) SM arose to improve the MMC's fault-blocking capability [71–74]. Table 6 illustrates the comparison of the salient features of the MMC SM topologies in terms of rating, operation, losses, design, and control complexity, as well as DC fault-blocking capability. For instance, the FB SM consists of four switches and one DC capacitor, where switching combinations result in three voltage levels: "0", "+V_c", and "-V_c". It has twice the number of switches as the HB SM for the same voltage rating, but the design and control complexities are similar. However, the two switching devices carry current during normal operation in the FB SM, causing higher power losses. The negative voltage levels in the FB SM are used to limit the current during DC-side fault scenarios.

Table 6. Comparison of MMC SM topologies [71].

Characteristic	HB	FB	CDC	3LCC FC
Number of Output Voltage Levels	2	3	4	3
Maximum Blocking Voltage of SM	V_c	V_c	$2 \times V_c$	$2 \times V_c$
Maximum Number of DC Capacitors Normalized to V_c	1	1	2	3
Number of Devices Normalized to V_c	2	4	7	4
Maximum Number of Devices in Conduction Path	1	2	3	2
Power Losses	Low	Moderate	High	Moderate
SM Design Complexity	Low	Low	High	High
SM Control Complexity	Low	Low	Low	High
Bipolar Operation?	No	Yes	Yes	No
DC Fault Blocking?	No	Yes	Yes	No

MMC control is generally challenging, as it entails multiple control objectives—namely, the capacitor voltage balancing control, circulating current control, and capacitor voltage ripple control. For reliable and safe operational control of the MMC, all of the control objectives must be optimal, amongst other aspects. Over the years, appropriate control/modulation schemes have emerged—as reviewed in [73,75]—to address MMC operational issues. Additionally, other issues such as modelling, SM topologies, fault diagnosis/tolerance, and protection have been investigated widely towards realizing an efficient MMC-based system [74–76].

The majority of MMC-based applications are largely for HB MMCs. For instance, the promising MMC proposed for VSC-HVDC application in [73] is based on the conventional HB SMs. However, this system faces the challenge of not blocking DC-side fault current due to its freewheeling diodes that allow uncontrollable flow of fault currents from AC and DC sources. Several converter topologies for limiting DC fault currents have been explored in the literature in favor of more innovative hybrid MMCs. In [77], an alternate arm converter is a hybrid MMC realized by combining FB SMs and a two-level VSC. The MMC is controlled to produce positive and negative half-cycles in the upper and lower arms, respectively; hence, each arm has a voltage rating equivalent to half of that of the HB MMC. The presence of the FB SMs enables the hybrid MMC to block DC fault currents during fault conditions. The authors of [78] proposed a hybrid MMC for MVDC application in which the upper and lower arms consist of series-connected HB SMs and FB SMs, respectively. Compared to the HB MMC, the hybrid MMC can produce the same voltage output quality at a lower cost. An innovative hybrid MMC with the number of FB modules reduced by about 10–20% was proposed in [79], with a DC capacitor in the fault-breaking circuit to block DC faults, whereas FB SMs only commutate the fault current from the FB MMC to the fault-breaking circuit. The proposal realized improved fault ride-through capability, with reduced capital costs and losses. The least cost hybrid MMC topology was proposed in [80], comprising HB SMs and only one FB SM in each lower arm, in addition to a four-step protection scheme. Figure 7 shows the innovative hybrid MMC structures.

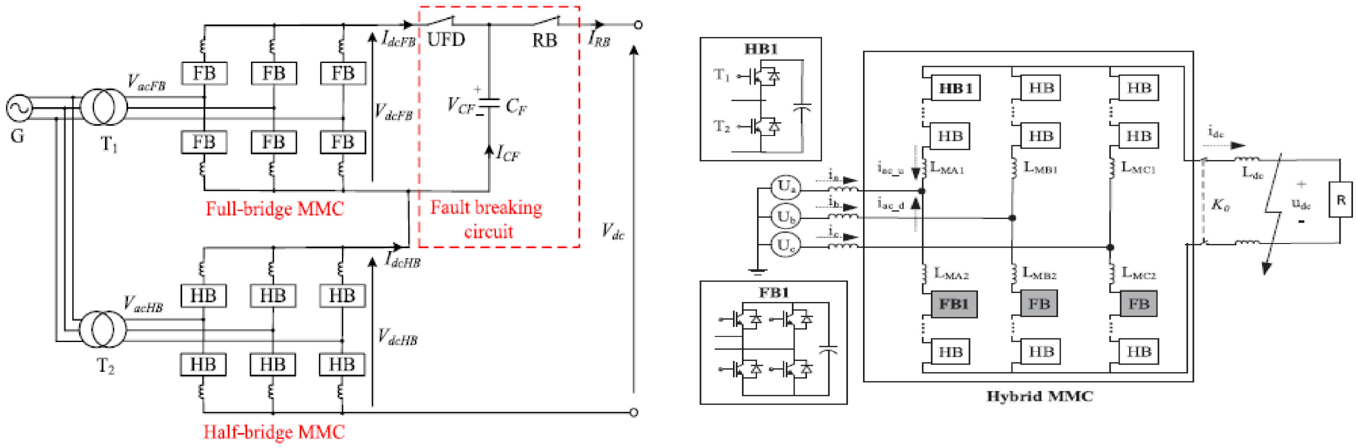

(**a**) (**b**)

Figure 7. Innovative hybrid MMCs: (**a**) with 10–20% FB SMs [79]; and (**b**) with only one FB SM in each lower arm [80].

The use of HB MMCs in TSS converters has already been demonstrated in key MVDC TPS studies, such as [7,10]. However, the vulnerability of HB MMCs—allowing the uncontrolled flow of DC fault currents—risks damaging all converters connected to the DC bus. The trends towards developing innovative and cost-effective hybrid MMC topology with HB SMs and fewer FB SMs is a potential option for use in MVDC TPSs for better performance and fault-blocking capability. A lot of research [73,76,81] has been undertaken on MMC modelling, topologies, control schemes, modulation strategies, fault diagnosis/tolerance, protection, and related challenges. From the analysis, some of the challenges include the unavailability of accurate and efficient SM/MMC models and limited insight into MMCs' internal dynamics, reliability, and DC protection issues—research on which is still in progress [74,75,82].

3.2.2. Power Electronic Transformers (PETs)

Traditionally, the MVAC TPS employs LFT-based technology operating at 50/60 Hz—too bulky and heavy for future railway rolling stock traction applications. Advancements in power conversion systems have led to the emergence of PET-based systems that are proving to be better in terms of power density, efficiency, power quality, and other additional functionalities—such as fault current limiting and isolation [33]. Figure 8 shows the power conversion systems; compared to the LFT system, an additional conversion stage is added in the case of the PET, and a direct interface of the active front-end (AFE) converter made to the OHL. Typically the AFEs are connected in series in order to enhance the maximum blocking voltage of the power electronic switches, while at the output a parallel connection is made to form an input-series-output-parallel (ISOP) configuration [64].

The early PET-based traction systems introduced from 1985 are summarized in Table 7.

From the above PET evolution trends, the availability of IGBTs in 1996 marked the development of the most practical PET, which was later deployed widely in traction applications. The design could withstand higher catenary voltage due to the ISOP configuration. The fully controllable IGBTs could facilitate bidirectional power flow. The soft switching characteristics considerably lowered the losses, improving efficiency, among other benefits. It is from these early concepts that major PET-based railway traction system development emerged.

A number of leading rolling stock manufacturers—such as Alstom, Siemens, Bombardier, and ABB—have made groundbreaking developments in PET research. Table 8 summarizes major PET developments for railway traction.

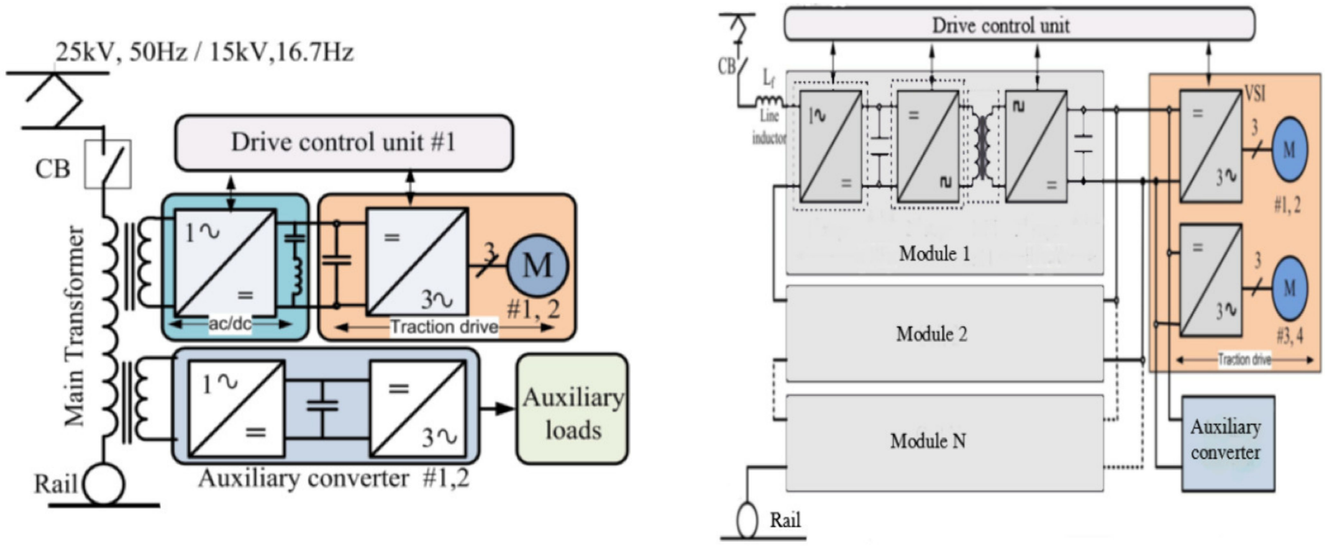

(**a**) (**b**)

Figure 8. Power conversion systems: (**a**) LFT-based and (**b**) PET-based.

Table 7. Early PET-based systems.

Year	Developer	MVAC TPS	Key PET Features
1985	University of Leoben, Austria	15 kV, 16 2/3 Hz	Thyristor-based: Input rectifier (no DC bus capacitor), a matrix converter, an MFT (400 Hz), an output rectifier, and a DC–DC booster converter for voltage regulation [33].
1993	Royal Institute of Technology, Sweden	15 kV, 16 2/3 Hz	Thyristor-based: FE converter natural commutation, an MFT, and a four-quadrant output converter (forced commutation) [83].
1996	Ecole Polytechnique Federale De Lausanne (EPFL), Switzerland	15 kV, 16 2/3 Hz	IGBT-based: Direct-coupled input four-quadrant multilevel converter with the OHLs; has reversible DC–DC converter with MF AC links, ISOP configuration, and soft switching [84].
1998	Siemens	15 kV, 16 2/3 Hz	IGBT-based: Cascaded H-bridge (CHB) modules, high-voltage IGBTs (6.5 kV), MFTs, soft switching, and ISOP configuration [33].
2001	ABB	15 kV, 16 2/3 Hz 25 kV, 50 Hz	Thyristors in [83] replaced by IGBTs: Single/three-phase [85].

Table 8. Major PET developments for railway traction.

Year	Developer/Key PET' Features	System Topology Excluding Traction Drive
2003	Alstom: Prototype of a 1500-kVA e-transformer for a 15-kV, 16-2/3-Hz MVAC TPS; 1st (hard switching) and 3rd stages a full H-bridge, 2nd stage (soft switching) a half H-bridge, MFT 5 kHz, 6.5-kV/400-A IGBTs and 3.3-kV/400-A IGBTs; 52 IGBTs total. Lower component count than other PETs [86].	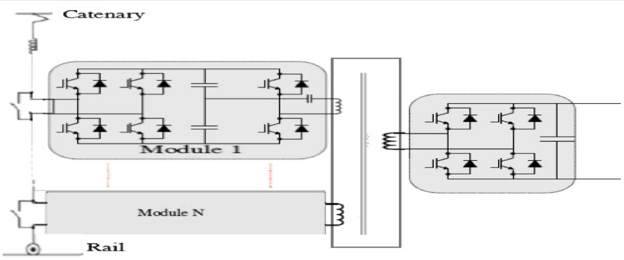

Table 8. *Cont.*

Year	Developer/Key PET' Features	System Topology Excluding Traction Drive
2004	Siemens: Prototype of a 2-MVA MMC structure for a 15-kV, 16-2/3-Hz MVAC TPS comprising a 17-level MMC with 1.2-kV/400-A IGBTs, 8 modules, and a 1-kHz MFT. Predicted efficiency of 98% [87].	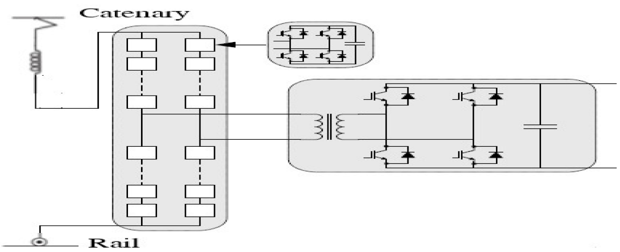
2007	Bombardier: Prototype of a 300-kVA, 8-kHz MFT for a 15-kV, 16-2/3-Hz MVAC TPS; all stages have full H-bridges, i.e., AC/DC, DC/AC; AC/DC, respectively; 96 6.5-kV IGBTs; power reduction by 12.5% [67].	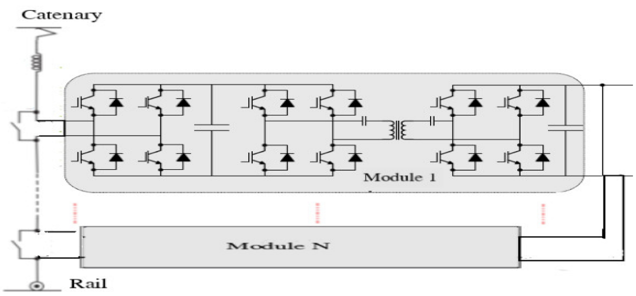
2007	ABB: First prototype for a 1200-kVA PET for a 15-kV, 16-2/3-Hz MVAC TPS; 2-stage multilevel AFE converter, 400-Hz MFT, 3.3-kV IGBTs, and 6.5-kV/400-A IGBTs,;192 IGBTs total; hence, slightly higher efficiency (3%) and higher component count than LFT [88].	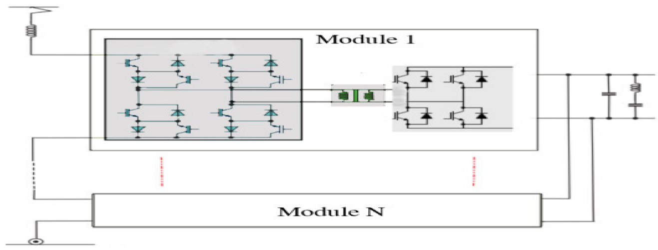
2012	ABB: Advanced 1200-kVA PET prototype for a 15-kV, 16-2/3-Hz MVAC TPS; 1st and 2nd stages a full H-bridge (6.5-kV/400-A IGBTs), 3rd a half H-bridge (3.3-kV/800-A IGBTs); MFT 400 Hz; 72 IGBTs total; 96% efficiency [33,89].	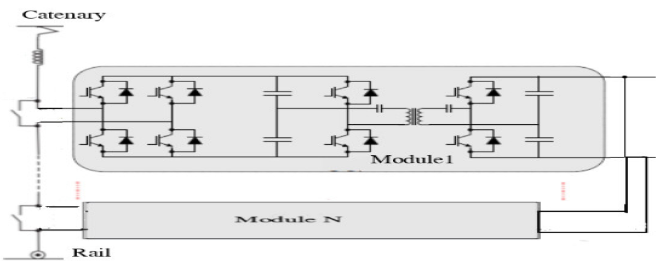
2014	ABB: 1.2-MVA PET prototype for a 15-kV, 16-2/3-Hz MVAC TPS; 1.75-Hz MFT, used 6.5-kV/400-A IGBTs and 3.3-kV/800-A IGBTs; cascaded multilevel front-end converter; tested on a locomotive in Geneva, Switzerland; success is a great milestone of the PET technology for railway traction applications [90].	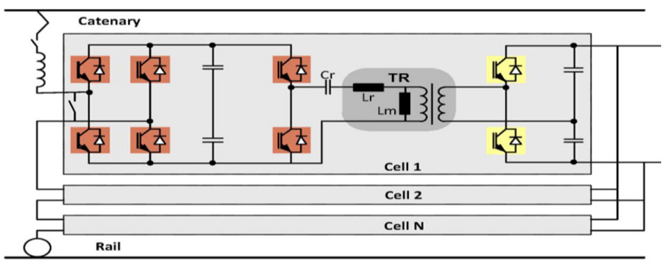

A preview of the evolution of PETs amongst the major rolling stock manufacturers shows increasing prospects for PET-based traction systems—especially for 15-kV, 16-2/3-Hz MVAC TPSs. The benefits of improved efficiency, energy savings, and weight/size reduction have been demonstrated. There is also the popularity of IGBT-based cascaded/modular ISOP configuration in the PET topology. Power converter topologies for PET-based traction systems are reviewed in [64], and MMCs are considered to be the topology of the future due to their modularity and fault-tolerant capabilities. Furthermore, [86] demonstrated an MMC-based PET with 98.2% efficiency. Discussions in [9] to upgrade the 1.5-kV DC TPS to a 9-kV MVDC in order to reduce catenary voltage drop and the number of TSSs inspired an MMC-based PET whose effectiveness required innovative MMC topology and DC protection schemes, as demonstrated in [80,91]. There are also great prospects for the emerging SiC devices extensively studied in [49] in place of the Si-IGBTs in MMC-based PETs, including advances in MFTs demonstrated in [33,63]. For example, a 3.6-kV/1.8-kV PET designed from 3.3-kV SiC MOSFETs with ISOP structures demonstrated good performance and 98.8% efficiency at 300 kW [8,92].

Most of the major PET models reviewed are largely modular-structured, with cascaded/modular ISOP configuration for the 15-kV, 16.7-Hz MVAC TPS. Some innovations in key PET models can be adapted for MVDC rolling stock application by modifying the input conversion stage. Although the MMC-based PET configuration is scalable to high voltages and power levels, increasing the component count and complexity raises reliability questions. The authors of [74] comment on how it is so challenging to accurately estimate and cost-effectively improve the reliability of the MMC-based systems. Some researchers acknowledge these reliability questions as the price for MMC-based systems' functionality beyond the conventional LFTs. However, one way of mitigating the reliability concerns is by reducing the mean time between failures, though this increases the PET complexity [90]. Considering the lifespan of LFTs—which is typically three times that of power converters—the total cost of ownership is lower for PETs, ignoring their potential savings from functionalities like weight/volume reduction, improved efficiency, etc. [24,89]. Future research on the quantification of PETs' system level impacts [89] may give a better insight into their costs. Finally, designing a PET involves exploring opposing constraints—such as optimizing power density as well as space/weight—when determining an effective thermal design. Realizing an effective thermal design principle that provides excellent performance is a challenging trade-off [33,93]. Advances in SiC devices as well as MFTs offer better future prospects for railway traction when challenges in thermal modelling, manufacturing process, reliability, etc. are fully addressed [33,64].

3.3. System Level

The concept of smart grids (SGs) has been trending worldwide as the vision for modernizing the electrical power grid infrastructure to meet future challenges. For instance, in the USA there has been a rapid increase in annual investments in SG infrastructure, with a rise from USD 3.4 billion in 2014 to USD 4.8 billion (41%) in 2016. This is projected to grow even further, to USD 13.8 billion in 2024 [94]. European SGs recorded about 89 completed projects, 8 of which had a total investment of EUR 60 million. In total, from 2002 to 2016, Europe had 467 SG projects across 47 countries under a budget of about EUR 3.75 billion [95]. The Asian region—led by China, Japan, and South Korea—increasingly invested in SG power infrastructure, to the tune of USD 11.9 billion to USD 28.8 billion between 2011 and 2017, respectively [96].

SG applications are predominantly in residential, commercial, and industrial sectors, where it is easy to predict the load demand. However, in the electric railway sector, there is very limited application of SGs, as the demand of the railway traction system varies significantly and is challenging to predict. For instance, a section of the TPS may carry multiple trains exhibiting variable loads depending on the train location, section gradient/curvature, and train operation profile. When braking, the train produces regenerative braking energy (RBE), which is dissimilar during traction, cruising, and coasting, and adds to the complexity [97]. Despite these complexities, railway SG (RSG) application has the potential to reduce reliance on fossil fuels by integrating RESs; hence, significant CO_2 emission reductions and increased supply reliability, encouraging railway companies to implement energy conservation measures such as demand-side management (DSM) to reduce costs as well as manage the stochastic nature of the rail traction demand. Additionally, RSGs can reduce energy consumption, hence reducing related costs, and can attract customers with increased reliability and help to future-proof supply against increased demand and uncertainties in availability and price [13].

The electric railway TPS is a unique, dedicated, and costly investment; hence, the application of SG principles therein is different from other sectors. In this way, many researchers have delved into aspects of integrating SG and microgrid technologies without a complete overhaul of the infrastructure. For instance, a study on the necessity and possibility of applying SG technology on the Japan East Railway in [98] centered on how eco-friendliness could be enhanced by exploring opportunities for the integration of rooftop PV to the DC TPSs—including MVAC TPSs for HSR applications — and the incorporation of power regeneration inverters at TSSs or ESSs to utilize RBE. Another study by the same railway company [99] demonstrated how maximum demand on a TSS as well as transformer capacity could be decreased when SG concepts are applied. One study [100] proposed a hybrid ESS for storing RBE and supplying auxiliary station loads to improve DC TPS efficiency; a more practical follow-up of the study [98] demonstrated the use of three SG-related technologies in DC and MVAC TPS—namely, effective use of RBE by means of reversible TSSs and ESSs; PV integration and power-conditioning systems, and DSM at the demand response TSSs and office buildings. The RSG technology proved effective in optimizing power consumption in the TPSs, with future potential for minimizing CO_2 emissions [101].

In order to realize the dramatic benefits of the RSG outlined in [13], effective controllability of the electric railway infrastructure is very important. Coordinated control of traffic flow and electrification would resolve various operational challenges—such as capacity constraints, energy costs, planned operation changes, etc.—including many other aspects that the traditional control schemes cannot manage [102]. A comprehensive TPS architecture integrating onboard and trackside ESSs, DERs, railway and external consumers (ECs), and RBE utilization incorporating intelligent substations (ISSTs), reversible substations (RSSTs); non-reversible substations (SSTs), and dynamic onboard energy managers (DOEMs) under the Merlin project by the European Commission serves as a classical RSG [103]. Its railway energy management system (REM-S) based on SG architecture was proposed in [37] and successfully implemented on a 3-kV DC Spanish railway system in [46]. Its centralized–decentralized RSG architecture demonstrated effective operational control as well as achievement of energy consumption, power demand, and energy cost optimization. Figure 9 displays the Merlin REM-S architecture.

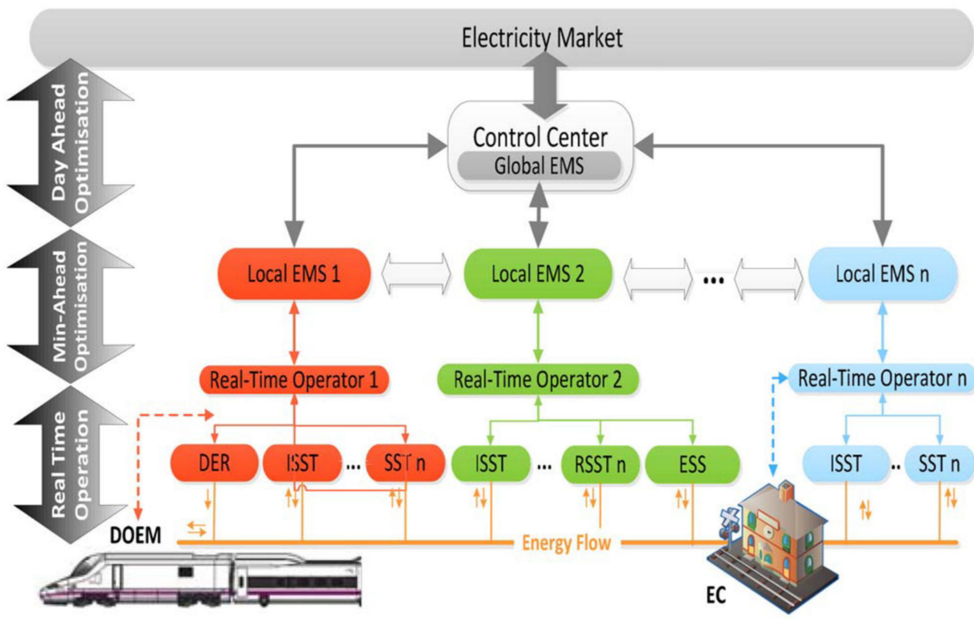

Figure 9. Merlin REM-S architecture [37].

The implementation of SGs to build new TPSs and reconstruct existing TPSs is a revolutionary step towards a sustainable railway sector in the future. The novel energy hub concept and integration of DERs in DC and AC railway microgrids is proposed in [14] for developing impressive capabilities and opportunities. With a specific focus on the DC railway microgrids, a DC energy hub established at the TSS level and/or mid-span of the TSSs can harvest massive amounts of power from DERs and RBE, as well as efficiently delivering internal and external loads with significant energy savings in the 0.6–3.0-kV DC TPSs, as well as the prospective MVDC TPSs. Despite the few studies on the MVDC TPS [12], it incorporates the advantages of both AC and DC microgrids, with immense benefits to the future energy hub, as shown in Figure 10 [14]. Although an REM-S is not proposed in [14], the architecture provided in the Merlin project can be adopted.

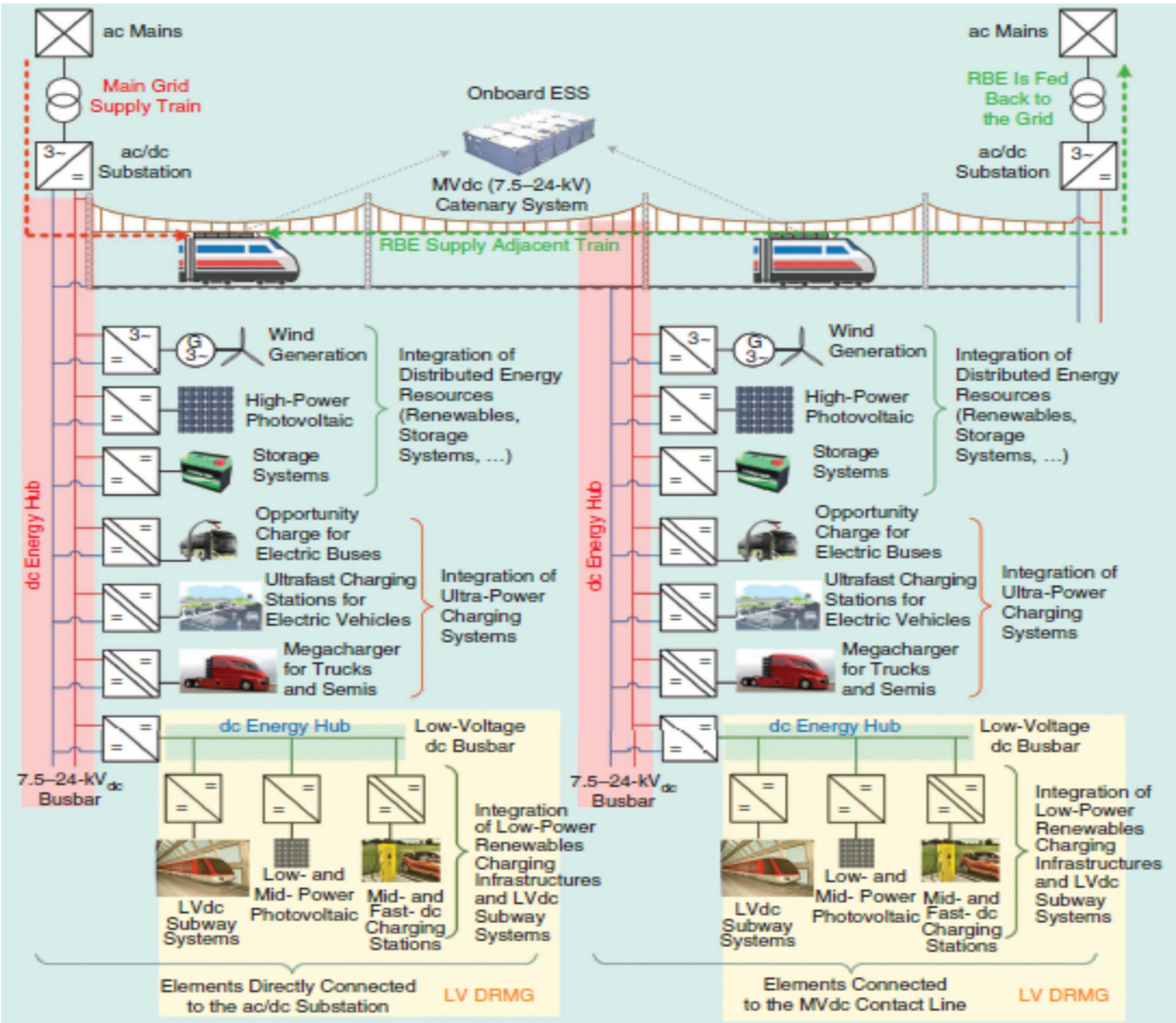

Figure 10. Future MVDC energy hub [14].

There are numerous opportunities for implementing SG technologies in electrical TPSs, including MVDC TPSs, given that they are among the largest and heaviest consumers of power in the utility grid [14,102]. RSGs offer an opportunity for the rail sector to cut down on CO_2 emissions, increase supply reliability, and incentivize railway companies into employing energy-saving measures, among other benefits. There are also barriers—for instance, the electrical railway TPS is a complex network with diverse loads and energy sources, necessitating a highly complex hierarchical control system. Thus, a new sophisticated supervisory control and data acquisition (SCADA) system is required for effective controllability. Table 9 summarizes RSG challenges and solutions [13].

Table 9. RSG railway challenges and solutions [13].

Challenges	Solutions
New equipment to achieve effective monitoring and controllability.	Distributed and networked SCADA systems with standardized protocols, unlike the traditional SCADA.
New signalling and communications system to guarantee quality service while the trains are moving through a range of environments, e.g, remote regions, tunnels, across networks, etc.	New railway signalling and communication; global system mobile communication railway (GSM-R) is a valuable case study for innovation.
DER integration issues, i.e., PV and wind intermittencies and site specificities, in addition to the rail traction load variability.	Systems approach in determining the type, number, size, and location of DERs for integration.
Data from multiple stakeholders and data processing.	Different sharing agreements and protocols by stakeholders to be redefined by the SG railway. Data feeds from different stakeholders with different notations for trains and stations to be standardized for SG railway management.
Cybersecurity against threats to signalling and communication systems.	Technical (a more robust cryptographic mechanism; a new key distribution scheme; a new key storage and system integrity module; and a set of countermeasures for avoiding radio jamming attacks) and policy (cybersecurity-related standards).
Standardisation and regulation.	Compliance is best practice for SG railway safety, as well as for technologies to be compatible and interoperable. Standards are necessary for monitoring and control devices; communication systems and protocols; EMC; cybersecurity; and data (collection, storage, and sharing).

4. Conclusions

The MVDC TPS is a promising electric railway infrastructure for future HSR transportation. However, as an emerging technology, it lacks two key pieces of mature power-converter-based equipment—namely, high-power traction converters, and PETs—to be competitive to the existing MVAC TPSs. However, the MVDC system can be a sustainable smart energy hub that offers power supply and related ancillary services in addition to traditional freight and passenger transportation. In this study, opportunities for developing the key equipment were explored in detail. A cost-effective hybrid MMC-based TSS converter, with HB SMs and one FB SM in each lower arm per phase, and an effective protection scheme, is available to enhance performance and capability against faults. Additionally, SiC MMC-based PETs in ISOP configuration exist for greater weight/size reduction and efficiency in MVDC rolling stock development. Finally, the concept of a smart MVDC infrastructure integrated with diverse loads and energy sources incorporating a sophisticated REM-S based on SG principles is the future for optimal MVDC TPS operation control, with numerous benefits. However, as a technology in the embryonic stages of development, there are knowledge gaps in various aspects—such as the new converter topology, regarding its reliability and protection issues—as well as high costs involved, in addition to lack of standardization. It is expected that as demand for railway electrification increases around the world, technology advances shall close the knowledge gaps, as well as stimulate cost reduction.

Author Contributions: Conceptualization, P.S. and I.E.D.; methodology, P.S.; formal analysis, P.S.; investigation, P.S.; resources, I.E.D.; writing—original draft preparation, P.S.; writing—review and editing, P.S.; visualization, P.S. and I.E.D.; supervision, I.E.D.; project administration, I.E.D.; funding acquisition, I.E.D. All authors have read and agreed to the published version of the manuscript.

Funding: This research received no external funding.

Acknowledgments: This work was supported by the Smartgrid Research Center, Durban University of Technology.

Conflicts of Interest: The authors declare no conflict of interest.

References

1. Bhargava, B. Railway electrification systems and configurations. In Proceedings of the 1999 IEEE Power Engineering Society Summer Meeting. Conference Proceedings (Cat. No.99CH36364), Edmonton, AB, Canada, 18–22 July 1999; Volume 1, pp. 445–450. [CrossRef]
2. Brenna, M.; Foiadelli, F.; Zaninelli, D. *Electrical Railway Transportation Systems*; John Wiley & Sons, Inc.: Hoboken, NJ, USA, 2018.
3. ABB. ABB, Powering the World's High-Speed Rail Networks. Available online: https://library.e.abb.com/public/3e14a09a05a47c17c12578f7005e8c8d/ABB-powering-%20the-worlds-high-speed-rail-network.pdf (accessed on 25 May 2021).
4. Laousse, D.; Paris, C.B.; Caron, H.; Courtois, C.; Denis, S. Direct current—A future under which conditions? *Elektr. Bahnen* **2016**, *114*, 260–275.
5. Steimel, A. Under Europe's Incompatible Catenary Voltages a Review of Multi-System Traction Technology. In Proceedings of the 2012 Electrical Systems for Aircraft, Railway and Ship Propulsion, Bologna, Italy, 16–18 October 2012; Institute of Electrical and Electronics Engineers (IEEE): New York, NY, USA, 2012.
6. Hinz, A.; Stieneker, M.; de Doncker, R.W. Impact and opportunities of medium-voltage DC grids in urban railway systems. In Proceedings of the 2016 18th European Conference on Power Electronics and Applications (EPE'16 ECCE Europe), Karlsruhe, Germany, 5–9 September 2016; Institute of Electrical and Electronics Engineers (IEEE): New York, NY, USA, 2016; pp. 1–10.
7. Gomez-Exposito, A.; Mauricio, J.M.; Maza-Ortega, J.M. VSC-Based MVDC Railway Electrification System. *IEEE Trans. Power Deliv.* **2013**, *29*, 422–431. [CrossRef]
8. Verdicchio, A.; Ladoux, P.; Caron, H.; Courtois, C. New Medium-Voltage DC Railway Electrification System. *IEEE Trans. Transp. Electrif.* **2018**, *4*, 591–604. [CrossRef]
9. Verdicchio, A.; Ladoux, P.; Caron, H.; Sanchez, S. Future DC Railway Electrification System—Go for 9 kV. In Proceedings of the 2018 IEEE International Conference on Electrical Systems for Aircraft, Railway, Ship Propulsion and Road Vehicles & International Transportation Electrification Conference (ESARS-ITEC), Nottingham, UK,, 7–9 November 2018; Institute of Electrical and Electronics Engineers (IEEE): New York, NY, USA, 2018; pp. 1–5.
10. Yang, X.; Hu, H.; Ge, Y.; Aatif, S.; He, Z.; Gao, S.; Salman, A. An Improved Droop Control Strategy for VSC-Based MVDC Traction Power Supply System. *IEEE Trans. Ind. Appl.* **2018**, *54*, 5173–5186. [CrossRef]
11. Aatif, S.; Hu, H.; Yang, X.; Ge, Y.; He, Z.; Gao, S. Adaptive droop control for better current-sharing in VSC-based MVDC railway electrification system. *J. Mod. Power Syst. Clean Energy* **2019**, *7*, 962–974. [CrossRef]
12. Arboleya, P.; Mayet, C.; Mohamed, B.; Aguado, J.A.; de la Torre, S. A review of railway feeding infrastructures: Mathematical models for planning and operation. *eTransportation* **2020**, *5*, 100063. [CrossRef]
13. Steele, H.; Roberts, C.; Hillmansen, S. Railway smart grids: Drivers, benefits and challenges. *Proc. Inst. Mech. Eng. Part F: J. Rail Rapid Transit* **2019**, *233*, 526–536. [CrossRef]
14. Brenna, M.; Foiadelli, F.; Kaleybar, H.J. The Evolution of Railway Power Supply Systems Toward Smart Microgrids: The concept of the energy hub and integration of distributed energy resources. *IEEE Electrif. Mag.* **2020**, *8*, 12–23. [CrossRef]
15. Leander, P.; Ostlund, S. A Concept for an HVDC Traction System. In Proceedings of the International Conference on Main Line Railway Electrification 1989, York, UK, 25–28 September 1989; IET: London, UK, 1989.
16. Abrahamsson, L.; Kjellqvist, T.; Ostlund, S. High-voltage DC-feeder solution for electric railways. *IET Power Electron.* **2012**, *5*, 1776–1784. [CrossRef]
17. Stieneker, M.; Mortimer, B.J.; Hinz, A.; Muller-Hellmann, A.; de Doncker, R.W. MVDC Distribution Grids for Electric Vehicle Fast-Charging Infrastructure. In Proceedings of the International Power Electronics Conference, Niigata, Japan, 20–24 May 2018; Institute of Electrical and Electronics Engineers (IEEE): New York, NY, USA, 2018.
18. Stieneker, M.; Doncker, R.W.D. Medium-voltage DC distribution grids in urban areas. In Proceedings of the IEEE 7th International Symposium on Power Electronics for Distributed Generation Systems (PEDG), Vancouver, BC, Canada, 27–30 June 2016; Institute of Electrical and Electronics Engineers (IEEE): New York, NY, USA, 2016.
19. Aatif, S.; Yang, X.; Hu, H.; Maharjan, S.K.; He, Z. Integration of PV and Battery Storage for Catenary Voltage Regulation and Stray Current Mitigation in MVDC Railways. *J. Mod. Power Syst. Clean Energy* **2021**, *9*, 585–594. [CrossRef]
20. Serrano-Jiménez, D.; Abrahamsson, L.; Castaño-Solís, S.; Sanz-Feito, J. Electrical railway power supply systems: Current situation and future trends. *Int. J. Electr. Power Energy Syst.* **2017**, *92*, 181–192. [CrossRef]

21. Shigeeda, H.; Morimoto, H.; Ito, K.; Fujii, T.; Morishima, N. Feeding-loss Reduction by Higher-voltage DC Railway Feeding System with DC-to-DC Converter. In Proceedings of the 2018 International Power Electronics Conference, Niigata, Japan, 20–24 May 2018; Institute of Electrical and Electronics Engineers (IEEE): New York, NY, USA, 2018.
22. Ferencz, I.; Petreus, D.; Tricoli, P. Converter Topologies for MVDC Traction Transformers. In Proceedings of the 2020 IEEE 26th International Symposium for Design and Technology in Electronic Packaging (SIITME), Pitesti, Romania, 21–24 October 2020; Institute of Electrical and Electronics Engineers (IEEE): New York, NY, USA, 2020; pp. 362–367.
23. Huber, J.E.; Kolar, J.W. Solid-State Transformers: On the Origins and Evolution of Key Concepts. *IEEE Ind. Electron. Mag.* **2016**, *10*, 19–28. [CrossRef]
24. Huber, J.E.; Kolar, J.W. Applicability of Solid-State Transformers in Today's and Future Distribution Grids. *IEEE Trans. Smart Grid* **2019**, *10*, 317–326. [CrossRef]
25. Giannakis, A.; Peftitsis, D. MVDC Distribution Grids and Potential Applications: Future Trends and Protection Challenges. In Proceedings of the 20th European Conference on Power Electronics and Applications (EPE'18 ECCE Europe), Riga, Latvia, 17–21 September 2018; Institute of Electrical and Electronics Engineers (IEEE): New York, NY, USA, 2018.
26. Pei, X.; Cwikowski, O.; Rodriguez, D.S.V.; Barnes, M.; Smith, A.; Shuttleworth, R. A review of technologies for MVDC circuit breakers. In Proceedings of the IECON 2016—42nd Annual Conference of the IEEE Industrial Electronics Society, Florence, Italy, 23–26 October 2016; Institute of Electrical and Electronics Engineers (IEEE): New York, NY, USA, 2016; pp. 3799–3805.
27. Siemens. *MVDC Plus—Managing the Future Grid*; Siemens AG: Munich, Germany, 2017; p. 8.
28. Zhu, R.; Liang, T.; Dinavahi, V.; Liang, G. Wideband Modeling of Power SiC mosfet Module and Conducted EMI Prediction of MVDC Railway Electrification System. *IEEE Trans. Electromagn. Compat.* **2020**, *62*, 2621–2633. [CrossRef]
29. Ghaviha, N.; Campillo, J.; Bohlin, M.; Dahlquist, E. Review of Application of Energy Storage Devices in Railway Transportation. *Energy Procedia* **2017**, *105*, 4561–4568. [CrossRef]
30. Khodaparastan, M.; Mohamed, A.A.; Brandauer, W. Recuperation of Regenerative Braking Energy in Electric Rail Transit Systems. *IEEE Trans. Intell. Transp. Syst.* **2019**, *20*, 2831–2847. [CrossRef]
31. Sparacino, A.R.; Grainger, B.M.; Kerestes, R.J.; Reed, G.F. Design and simulation of a DC electric vehicle charging station connected to a MVDC infrastructure. In Proceedings of the 2012 IEEE Energy Conversion Congress and Exposition (ECCE), Raleigh, NC, USA, 15–20 September 2012; Institute of Electrical and Electronics Engineers (IEEE): New York, NY, USA, 2012; pp. 1168–1175.
32. Wang, Y.; Zheng, Z.; Li, Y. DAB-based PET in MVDC traction and shipboard applications with distribution and redundant control. *J. Eng.* **2018**, *20*, 3209–3213.
33. Feng, J.; Chu, W.; Zhang, Z.; Zhu, Z. Power Electronic Transformer-Based Railway Traction Systems: Challenges and Opportunities. *IEEE J. Emerg. Sel. Top. Power Electron.* **2017**, *5*, 1237–1253. [CrossRef]
34. Hammerstrom, D.J. AC Versus DC Distribution Systems, Did We Get it Right? In Proceedings of the 2007 IEEE Power Engineering Society General Meeting, Tampa, FL, USA, 24–28 June 2007; Institute of Electrical and Electronics Engineers (IEEE): New York, NY, USA, 2007.
35. Sannino, A.; Postiglione, G.; Bollen, M. Feasibility of a DC network for commercial facilities. *IEEE Trans. Ind. Appl.* **2003**, *39*, 1499–1507. [CrossRef]
36. Nilsson, D.; Sannino, A. Efficiency analysis of low- and medium-voltage dc distribution systems. In Proceedings of the Eighth IEEE International Symposium on Spread Spectrum Techniques and Applications—Programme and Book of Abstracts (IEEE Cat. No.04TH8738), Denver, CO, USA, 6–10 June 2004; Institute of Electrical and Electronics Engineers (IEEE): New York, NY, USA, 2005; Volume 2, pp. 2315–2321.
37. Khayyam, S.; Ponci, F.; Goikoetxea, J.; Recagno, V.; Bagliano, V.; Monti, A. Railway Energy Management System: Centralized–Decentralized Automation Architecture. *IEEE Trans. Smart Grid* **2015**, *7*, 1164–1175. [CrossRef]
38. Gran, R.J. *Numerical Computing with Simulink, Volume I: Creating Simulations*; Society for Industrial and Applied Mathematics: Philadelphia, PA, USA, 2007.
39. Simiyu, P.; Xin, A.; Bitew, G.T.; Shahzad, M.; Kunyu, W.; Tuan, L.K. Review of the DC voltage coordinated control strategies for multi-terminal VSC-MVDC distribution network. *J. Eng.* **2019**, *2019*, 1462–1468. [CrossRef]
40. Gao, F.; Bozhko, S.; Asher, G.; Wheeler, P.; Patel, C. An Improved Voltage Compensation Approach in A Droop-Controlled DC Power System for the More Electric Aircraft. *IEEE Trans. Power Electron.* **2015**, *31*, 1. [CrossRef]
41. Dragicevic, T.; Lu, X.; Vasquez, J.C.; Guerrero, J.M. DC Microgrids–Part I: A Review of Control Strategies and Stabilization Techniques. *IEEE Trans. Power Electron.* **2015**, *31*, 4876–4891. [CrossRef]
42. Rouzbehi, K.; Miranian, A.; Luna, A.; Rodriguez, P. DC Voltage Control and Power Sharing in Multiterminal DC Grids Based on Optimal DC Power Flow and Voltage-Droop Strategy. *IEEE J. Emerg. Sel. Top. Power Electron.* **2014**, *2*, 1171–1180. [CrossRef]
43. Gavriluta, C.; Candela, I.; Luna, A.; Gomez-Exposito, A.; Rodriguez, P. Hierarchical Control of HV-MTDC Systems With Droop-Based Primary and OPF-Based Secondary. *IEEE Trans. Smart Grid* **2014**, *6*, 1502–1510. [CrossRef]
44. Simiyu, P.; Xin, A.; Wang, K.; Adwek, G.; Salman, S. Multiterminal Medium Voltage DC Distribution Network Hierarchical Control. *Electronics* **2020**, *9*, 506. [CrossRef]
45. Hao, F.; Zhang, G.; Chen, J.; Liu, Z.; Xu, D.; Wang, Y. Optimal Voltage Regulation and Power Sharing in Traction Power Systems with Reversible Converters. *IEEE Trans. Power Syst.* **2020**, *35*, 2726–2735. [CrossRef]

46. Khayyam, S.; Berr, N.; Razik, L.; Fleck, M.; Ponci, F.; Monti, A. Railway System Energy Management Optimization Demonstrated at Offline and Online Case Studies. *IEEE Trans. Intell. Transp. Syst.* **2018**, *19*, 3570–3583. [CrossRef]
47. Razik, L.; Berr, N.; Khayyam, S.; Ponci, F.; Monti, A.; Khayyamim, S. REM-S–Railway Energy Management in Real Rail Operation. *IEEE Trans. Veh. Technol.* **2018**, *68*, 1266–1277. [CrossRef]
48. Wang, F.; Zhang, Z.; Jones, E.A. *Characterization of Wide Bandgap Power Semiconductor Devices*; IET: London, UK, 2018.
49. Das, S.; Marlino, L.D.; Armstrong, K.O. Wide Bandgap Semiconductor Opportunities in Power Electronics. Technical Report ORNL/TM-2017/702. 2017. Available online: https://www.osti.gov/biblio/1415915/ (accessed on 30 May 2021).
50. Millan, J.; Godignon, P.; Perpiñà, X.; Perez-Tomas, A.; Rebollo, J. A Survey of Wide Bandgap Power Semiconductor Devices. *IEEE Trans. Power Electron.* **2014**, *29*, 2155–2163. [CrossRef]
51. Armstrong, K.O.; Das, S.; Cresko, J. Wide bandgap semiconductor opportunities in power electronics. In Proceedings of the IEEE 4th Workshop on Wide Bandgap Power Devices and Applications (WiPDA), Fayetteville, AR, USA, 7–9 November 2016; Institute of Electrical and Electronics Engineers (IEEE): New York, NY, USA, 2016.
52. Chow, T.P. Wide bandgap semiconductor power devices for energy efficient systems. In Proceedings of the 2015 IEEE 3rd Workshop on Wide Bandgap Power Devices and Applications (WiPDA), Blacksburg, VA, USA, 2–4 November 2015; Institute of Electrical and Electronics Engineers (IEEE): New York, NY, USA, 2015; pp. 402–405.
53. Das, M.K.; Capell, C.; Grider, D.E.; Leslie, S.; Ostop, J.; Raju, R.; Schutten, M.; Nasadoski, J.; Hefner, A. 10 kV, 120 A SiC half H-bridge power MOSFET modules suitable for high frequency, medium voltage applications. In Proceedings of the 2011 IEEE Energy Conversion Congress and Exposition, Phoenix, AZ, USA, 17–22 September 2011; Institute of Electrical and Electronics Engineers (IEEE): New York, NY, USA, 2011; pp. 2689–2692.
54. Hamada, K.; Hino, S.; Miura, N.; Watanabe, H.; Nakata, S.; Suekawa, E.; Ebiike, Y.; Imaizumi, M.; Umezaki, I.; Yamakawa, S. 3.3 kV/1500 A power modules for the world's first all-SiC traction inverter. *Jpn. J. Appl. Phys.* **2015**, *54*, 4DP07. [CrossRef]
55. Sato, K.; Kato, H.; Fukushima, T. Development of SiC Applied Traction System for Shinkansen High-speed Train. In Proceedings of the 2018 International Power Electronics Conference, Niigata, Japan, 20–24 May 2018; Institute of Electrical and Electronics Engineers (IEEE): New York, NY, USA, 2018.
56. Huang, A.Q.; Wang, L.; Tian, Q.; Zhu, Q.; Chen, D.; Wensong, Y. Medium voltage solid state transformers based on 15 kV SiC MOSFET and JBS diode. In Proceedings of the IECON 2016—42nd Annual Conference of the IEEE Industrial Electronics Society, Florence Italy, 23–26 October 2016; Institute of Electrical and Electronics Engineers (IEEE): New York, NY, USA, 2016; pp. 6996–7002.
57. Vechalapu, K.; Bhattacharya, S.; van Brunt, E.; Ryu, S.-H.; Grider, D.; Palmour, J.W. Comparative evaluation of 15 kV SiC MOSFET and 15 kV SiC IGBT for medium voltage converter under same dv/dt conditions. *IEEE J. Emerg. Sel. Top. Power Electron.* **2015**, *5*, 927–934. [CrossRef]
58. Pala, V.; van Brunt, E.; Cheng, L.; Oloughlin, M.J.; Richmond, J.; Burk, A.; Allen, S.T.; Grider, D.; Palmour, J.W.; Scozzie, C.J. 10 kV and 15 kV silicon carbide power MOSFETs for next-generation energy conversion and transmission systems. In Proceedings of the 2014 IEEE Energy Conversion Congress and Exposition (ECCE), Pittsburgh, PA, USA, 14–18 September 2014; Institute of Electrical and Electronics Engineers (IEEE): New York, NY, USA, 2014; pp. 449–454.
59. Hitachi. Hitachi IGBT Status List. 2021. Available online: https://www.hitachi-power-semiconductor-device.co.jp/en/products/igbt/pdf/ig13_eR3_2021_03.pdf (accessed on 20 May 2021).
60. Toshiba. Comparison of SiC MOSFET and Si IGBT. 2020. Available online: https://toshiba.semicon-storage.com/info/docget.jsp?did=69799 (accessed on 20 May 2021).
61. Yu, J.; Burgos, R.; Mehrabadi, N.R.; Boroyevich, D. DC fault current control of modular multilevel converter with SiC-based Power Electronics Building Blocks. In Proceedings of the IEEE Electric Ship Technologies Symposium (ESTS), Arlington, VA, USA, 14–17 August 2017; Institute of Electrical and Electronics Engineers (IEEE): New York, NY, USA, 2017.
62. Agheb, E.; Hoidalen, H.K. Medium frequency high power transformers, state of art and challenges. In Proceedings of the 2012 International Conference on Renewable Energy Research and Applications (ICRERA), Nagasaki, Japan, 11–14 November 2012; Institute of Electrical and Electronics Engineers (IEEE): New York, NY, USA, 2012; pp. 1–6.
63. Garcia, R.; Escobar-Mejia, A.; George, K.; Balda, J.C. Loss comparison of selected core magnetic materials operating at medium and high frequencies and different excitation voltages. In Proceedings of the 2014 IEEE 5th International Symposium on Power Electronics for Distributed Generation Systems (PEDG), Galway, Ireland, 24–27 June 2014; Institute of Electrical and Electronics Engineers (IEEE): New York, NY, USA, 2014; pp. 1–6.
64. Ronanki, D.; Williamson, S.S. Evolution of Power Converter Topologies and Technical Considerations of Power Electronic Transformer-Based Rolling Stock Architectures. *IEEE Trans. Transp. Electrif.* **2017**, *4*, 211–219. [CrossRef]
65. Ortiz, G.; Biela, J.; Kolar, J.W. Optimized design of medium frequency transformers with high isolation requirements. In Proceedings of the IECON 2010—36th Annual Conference on IEEE Industrial Electronics Society, Glendale, AZ, USA, 7–10 November 2010; Institute of Electrical and Electronics Engineers (IEEE): New York, NY, USA, 2010; pp. 631–638.
66. Leibl, M.; Ortiz, G.; Kolar, J.W. Design and Experimental Analysis of a Medium-Frequency Transformer for Solid-State Transformer Applications. *IEEE J. Emerg. Sel. Top. Power Electron.* **2017**, *5*, 110–123. [CrossRef]
67. Steiner, M.; Reinold, H. Medium frequency topology in railway applications. In Proceedings of the 2007 European Conference on Power Electronics and Applications, Aalborg, Denmark, 2–5 September 2007; Institute of Electrical and Electronics Engineers (IEEE): New York, NY, USA, 2007; pp. 1–10.

68. Zhao, C.; Lewedeni-Schmid, S.; Steinke, J.K.; Weiss, M.; Chaudhuri, T.; Pellerin, M.; Duron, J.; Stefanutti, P. Design, implementation and performance of a modular power electronic transformer (PET) for railway application. In Proceedings of the 14th European Conference on Power Electronics and Applications, Birmingham, UK, 30 August–1 September 2011; Institute of Electrical and Electronics Engineers (IEEE): New York, NY, USA, 2011.
69. Manoloiu, A.; Pereira, H.A.; Teodorescu, R.; Bongiorno, M.; Eremia, M.; Silva, S.R.; Alisa, M. Comparison of PI and PR current controllers applied on two-level VSC-HVDC transmission system. In Proceedings of the 2015 IEEE Eindhoven PowerTech, Eindhoven, The Netherlands, 29 June–2 July 2015; Institute of Electrical and Electronics Engineers (IEEE): New York, NY, USA, 2015.
70. Gelman, V. Insulated-Gate Bipolar Transistor Rectifiers: Why They Are Not Used in Traction Power Substations. *IEEE Veh. Technol. Mag.* **2014**, *9*, 86–93. [CrossRef]
71. Du, S.; Dekka, A.; Wu, B.; Zargari, N. *Modular Multilevel Converters: Analysis, Control, and Applications*; Wiley: Hoboken, NJ, USA, 2017.
72. Jing, T.; Maklakov, A.S. A Review of Voltage Source Converters for Energy Applications. In Proceedings of the Ural Conference on Green Energy (UralCon) 2018 International, Chelyabinsk, Russia, 4–6 October 2018; pp. 275–281.
73. Debnath, S.; Qin, J.; Bahrani, B.; Saeedifard, M.; Barbosa, P. Operation, Control, and Applications of the Modular Multilevel Converter: A Review. *IEEE Trans. Power Electron.* **2015**, *30*, 37–53. [CrossRef]
74. Zhang, L.; Arizona State University; Zou, Y.; Yu, J.; Qin, J.; Vijay, V.; Karady, G.G.; Shi, D.; Wang, Z.; America, G.N. Modeling, control, and protection of modular multilevel converter-based multi-terminal HVDC systems: A review. *CSEE J. Power Energy Syst.* **2017**, *3*, 340–352. [CrossRef]
75. Ronanki, D.; Williamson, S.S. Modular Multilevel Converters for Transportation Electrification: Challenges and Opportunities. *IEEE Trans. Transp. Electrif.* **2018**, *4*, 399–407. [CrossRef]
76. Deng, F.; Lu, Y.; Liu, C.; Heng, Q.; Yu, Q.; Zhao, J. Overview on submodule topologies, modeling, modulation, control schemes, fault diagnosis, and tolerant control strategies of modular multilevel converters. *Chin. J. Electr. Eng.* **2020**, *6*, 1–21. [CrossRef]
77. Merlin, M.; Green, T.; Mitcheson, P.D.; Trainer, D.R.; Critchley, R.; Crookes, W.; Hassan, F. The Alternate Arm Converter: A New Hybrid Multilevel Converter With DC-Fault Blocking Capability. *IEEE Trans. Power Deliv.* **2014**, *29*, 310–317. [CrossRef]
78. Wang, C.; Yang, Y.; Zhu, P. A Hybrid Modular Multilevel Converter (MMC) for MVDC Application. In Proceedings of the 2019 10th International Conference on Power Electronics and ECCE Asia (ICPE 2019—ECCE Asia), Busan, Korea, 27–30 May 2019; Institute of Electrical and Electronics Engineers (IEEE): New York, NY, USA, 2019.
79. Li, R.; Xu, L.; Yu, L.; Yao, L. A Hybrid Modular Multilevel Converter with Reduced Full-Bridge Submodules. *IEEE Trans. Power Deliv.* **2019**, *35*, 1876–1885. [CrossRef]
80. Huang, X.; Qi, L.; Pan, J. A New Protection Scheme for MMC-Based MVdc Distribution Systems with Complete Converter Fault Current Handling Capability. *IEEE Trans. Ind. Appl.* **2019**, *55*, 4515–4523. [CrossRef]
81. Sharifabadi, K.; Harnefors, L.; Nee, H.P.; Norrga, S.; Teodorescu, R. *Design, Control, and Application of Modular Multilevel Converters for HVDC Transmission Systems*; IEEE: New York, NY, USA, 2016; pp. 7–59.
82. Perez, M.A.; Ceballos, S.; Konstantinou, G.; Pou, J.; Aguilera, R.P. Modular Multilevel Converters: Recent Achievements and Challenges. *IEEE Open J. Ind. Electron. Soc.* **2021**, *2*, 224–239. [CrossRef]
83. Ostlund, S. Reduction of transformer rated power and line current harmonics in a primary switched converter system for traction applications. In Proceedings of the Fifth European Conference on Power Electronics and Applications, Brighton, UK, 13–16 September 1993; IET: London, UK.
84. Rufer, A.; Schibli, N.; Briguet, C. A direct coupled 4-quadrant multilevel converter for 16 2/3 Hz traction systems. In Proceedings of the Sixth International Conference on Power Electronics and Variable Speed Drives (Conf. Publ. No. 429), Nottingham, UK, 23–25 September 1996.
85. Kjaer, P.C.; Norrga, S.; Ostlund, S. A primary-switched line-side converter using zero-voltage switching. *IEEE Trans. Ind. Appl.* **2001**, *37*, 1824–1831. [CrossRef]
86. Farnesi, S.; Marchesoni, M.; Passalacqua, M.; Vaccaro, L. Solid-State Transformers in Locomotives Fed through AC Lines: A Review and Future Developments. *Energies* **2019**, *12*, 4711. [CrossRef]
87. Glinka, M. Prototype of multiphase modular-multilevel-converter with 2 MW power rating and 17-level-output-voltage. In Proceedings of the 2004 IEEE 35th Annual Power Electronics Specialists Conference (IEEE Cat. No.04CH37551), Aachen, Germany, 20–25 June 2014; Institute of Electrical and Electronics Engineers (IEEE): New York, NY, USA, 2004.
88. Hugo, N.; Stefanutti, P.; Pellerin, M.; Akdağ, A. Power electronics traction transformer. In Proceedings of the 2007 European Conference on Power Electronics and Applications, Aalborg, Denmark, 2–5 September 2007; Institute of Electrical and Electronics Engineers (IEEE): New York, NY, USA, 2007; pp. 1–10.
89. Dujic, D.; Kieferndorf, F.; Canales, F.; Drofenik, U. Power electronic traction transformer technology. In Proceedings of the Proceedings of the 7th International Power Electronics and Motion Control Conference, Habin, China, 2–5 June 2012; Institute of Electrical and Electronics Engineers (IEEE): New York, NY, USA, 2012; Volume 1, pp. 636–642.
90. Zhao, C.; Dujic, D.; Mester, A.; Steinke, J.K.; Weiss, M.; Lewdeni-Schmid, S.; Chaudhuri, T.; Stefanutti, P. Power Electronic Traction Transformer—Medium Voltage Prototype. *IEEE Trans. Ind. Electron.* **2014**, *61*, 3257–3268. [CrossRef]

91. Camurca, L.; Langwasser, M.; Zhu, R.; Liserre, M. Future MVDC Applications Using Modular Multilevel Converter. In Proceedings of the 2020 6th IEEE International Energy Conference (ENERGYCon), Gammarth, Tunisia, 28 September–1 October 2020; Institute of Electrical and Electronics Engineers (IEEE): New York, NY, USA, 2020; pp. 1024–1029.
92. Fabre, J.; Ladoux, P.; Caron, H.; Verdicchio, A.; Blaquiere, J.-M.; Flumian, D.; Sanchez, S. Characterization and Implementation of Resonant Isolated DC/DC Converters for Future MVdc Railway Electrification Systems. *IEEE Trans. Transp. Electrif.* **2021**, *7*, 854–869. [CrossRef]
93. Ronanki, D.; Williamson, S.S. Topological Overview on Solid-state Transformer Traction Technology in High-speed Trains. In Proceedings of the 2018 IEEE Transportation Electrification Conference and Expo (ITEC), Long Beach, CA, USA, 13–15 June 2018; Institute of Electrical and Electronics Engineers (IEEE): New York, NY, USA, 2018; pp. 32–37.
94. US Department of Energy. Smart Grid System Report. 2018; p. 93. Available online: https://www.energy.gov/sites/prod/files/2019/02/f59/Smart%20Grid%20System%20Report%20November%202018_1.pdf (accessed on 8 May 2021).
95. IqtiyaniIlham, N.; Hosenuzzaman, M. European smart grid prospects, policies, and challenges. *Renew. Sustain. Energy Rev.* **2017**, *67*, 776–790. [CrossRef]
96. Reza, M.M.A.; Hyder, T.; Rahman, M.M.; Shahriar, A. An Overview of Smart Grid Technology with its Present Situation and Anticipation in the Asian Region. *Eng. Int.* **2014**, *2*, 79–86. [CrossRef]
97. Sunghee, C. A study of smart grids for railways. Master's Thesis, School of Electrical & Electronic and System Engineering, University of Birmingham, Birmingham, UK, 2018.
98. Hayashiya, H.; Yoshizumi, H.; Suzuki, T.; Furukawa, T.; Kondoh, T.; Kitano, M.; Aoki, T.; Ishii, T.; Kurosawa, N.; Miyagawa, T. Necessity and possibility of smart grid technology application on railway power supply system. In Proceedings of the 14th European Conference on Power Electronics and Applications, Birmingham, UK, 30 August–1 September 2011.
99. Watanabe, Y.; Kaito, T.; Okuda, R.; Minamoto, M.; Kurosawa, N.; Hayashiya, H.; Yoshizumi, H. Examination on application of a smart grid technology to stations. In Proceedings of the 2012 15th International Power Electronics and Motion Control Conference (EPE/PEMC); Institute of Electrical and Electronics Engineers (IEEE): New York, NY, USA, 2012; p. DS2.d.11–1.
100. Nasr, S.; Iordache, M.; Petit, M. Smart micro-grid integration in DC railway systems. In Proceedings of the IEEE PES Innovative Smart Grid Technologies, Europe, Istanbul, Turkey, 12–15 October 2014; Institute of Electrical and Electronics Engineers (IEEE): New York, NY, USA, 2014; pp. 1–6.
101. Sekijima, S.; Sato, H.; Hayashiya, H. Application of Smartgrid Technology to Railway Power Supply. Technical Review, JR East. 2020, p. 40. Available online: https://www.jreast.co.jp/e/development/tech/pdf_40/tec-40-17-22eng.pdf (accessed on 23 May 2021).
102. De la Fuente, E.P.; Mazumder, S.K.; Franco, I.G. Railway Electrical Smart Grids: An introduction to next-generation railway power systems and their operation. *IEEE Electrif. Mag.* **2014**, *2*, 49–55. [CrossRef]
103. EU. Sustainable and Intelligent Management of Energy for Smarter Railway Systems in Europe: An Integrated Optimisation Approach. 2015. Available online: https://cordis.europa.eu/project/id/314125 (accessed on 15 May 2021).